

1. Attempts to Prepare Porous Materials Based on Thiols and Fluorinated Precursors

2. Self-sorting of Complex Libraries during Kinetically Controlled Acylations

A Thesis Presented to

the Faculty of the Department of Chemistry

University of Houston

In Partial Fulfillment

of the Requirements for the Degree

Master of Science

By

Xiao Liang

August 2015

1. Attempts to Prepare Porous Materials Based on Thiols and Fluorinated Precursors

2. Self-sorting of Complex Libraries during Kinetically Controlled Acylations

Xiao Liang

Dr. Ognjen Š. Miljanić, Chairman

Dr. Chengzhi Cai

Dr. Don Coltart

Dr. Shoujun Xu

Dr. Jacinta Conrad

Dean, College of Natural Sciences and
Mathematics

ACKNOWLEDGMENTS

Immeasurable appreciation and deepest gratitude for the help and support are extended to the following persons who in one way or another have contributed in making this thesis possible.

First, I would like to express my deepest appreciation to my advisor Dr. Ognjen Š Miljanić for accepting me into his group. He provides me an atmosphere of learning and research under his guidance, caring, and most importantly, his understanding. He also shared a lot of his knowledge and experience with me, and encouraged me to grow as an independent thinker instead of only a chemist, which I do not have enough words to express my deepest and sincere appreciation. I sincerely want to say thank you for everything you have done for me.

I wish to thank each colleague from the Miljanić group, Dr. Jaebum Lim, Dr. Teng-Hao Chen (Peter), Dr. Musabbir Saeed, Dr. Ljubodrag Vujisić, Dr. Merry Smith, Rio, Qing, Ha, Minyoung, Maxim, Chia-Wei, Mohammed, and Nadia for their numerous conversations, questions and help. I also want to thank Jennifer, Po-An (Alan), Lu, and numerous other friends outside this group for the time working with me. They are friends and co-workers that not only provided help, but also provided for some much needed humor and entertainment in what could have otherwise been a somewhat stressful laboratory environment.

I would also like to express my sincere gratitude to all of my family members for their support, encouragement and love. I must express my very profound gratitude to my

girlfriend Ling Bai. Her company, unfailing support, patience and unwavering love were undeniable. I thank my parents, Mei and Yunsheng, for their faith in me, allowing me to act on my ambitions. This accomplishment would not have been possible without them.

Finally, I would like to acknowledge my committee members Dr. Chengzhi Cai, Dr. Don Coltart, Dr. Shoujun Xu, and Dr. Jacinta Conrad for their respective comments and suggestions, as they are able to see my work from a different perspective.

Financial support provided by the National Science Foundation and Robert A. Welch Foundation are also gratefully appreciated.

1. Attempts to Prepare Porous Materials Based on Thiols and Fluorinated Precursors

2. Self-sorting of Complex Libraries during Kinetically Controlled Acylations

A Thesis Presented to

the Faculty of the Department of Chemistry

University of Houston

In Partial Fulfillment

of the Requirements for the Degree

Master of Science

By

Xiao Liang

August 2015

ABSTRACT

This thesis presents three studies in supramolecular chemistry. First is the synthesis and characterization of dynamic covalent disulfide bond based metal-organic framework (MOF), second is development of the fluorinated and imine-based non-covalent organic framework (nCOF), and the third is of molecular recognition between nucleophiles and acyl chlorides.

Chapter One follows the ligand design and post-synthetic tailoring as the two most important strategies in synthesizing new metal-organic frameworks (MOFs). Organic dynamic covalent ligand 4,4'-dithiobisbenzoic acid (DTBA) was designed to synthesize a new MOF with metal Cu. These new Cu-DTBA MOF crystals were then tested by reduction on reversible disulfide moieties in the organic ligand but the resulting product could not be further recrystallized. Cu-DTBA templated inter-molecular self-sorting between two disulfide ligands could be achieved successfully, but intra-molecular self-sorting from the single cross-linked disulfide ligand produced a different type of material which did not show the exchangeability of disulfide bonds.

Chapter Two shows the development of the nCOFs' structures based on the previous trispyrazole nCOF studies. The necessity of the terminal pyrazole and its trigonal ligand topology were confirmed by synthesizing and characterizing the following two nCOFs. Partially fluorinated trisphenyl nCOF replaced the terminal pyrazole by phenyl ring, which eliminated the hydrogen bonding, as well as linear imine-based nCOF which formed a different topology. The single crystal X-ray result of the two showed a

three-dimensional infinite network structure, but with very little voids that cannot be useful as porous solids.

Chapter Three introduces the simultaneous ordering and categorizing processes, i.e., self-sorting, which can occur under both thermodynamic and kinetic control. Thermodynamically controlled self-sorting phenomena widely exist in nature, while kinetically controlled self-sorting usually requires stimuli to help simplify the complex. Therefore, acylations between nucleophiles and acyl chlorides as fully kinetically controlled self-sorting systems were conducted. A series of [2×2] systems was conducted in order to find reactivity differences among nucleophiles as well as acyl chlorides. Furthermore, nine successful [3×3] systems achieved successful self-sorting with high selectivity.

TABLE OF CONTENTS

Chapter One Attempted Incorporation of Thiolate Ligands into Metal-Organic Frameworks

1.1	Introduction	1
1.1.1	Introduction to Metal Organic Frameworks (MOFs).....	1
1.1.2	Introduction to Disulfide Exchange	3
1.2	Results and Discussion.....	5
1.2.1	Preparation of a MOF from 4,4'-Dithiobisbenzoic Acid.....	5
1.2.2	X-ray Crystal Structure Analysis of Cu-DTBA MOF	6
1.2.3	Attempted Reduction and Recrystallization of MOF Crystals.....	9
1.2.4	Copper-Catalyzed Self-sorting between Disulfide Ligands	10
1.3	Experimental Section.....	12
1.3.1	General Procedures	12
1.3.2	Synthesis of 4-Mercaptobenzoic Acid (4)	13
1.3.3	Synthesis of 4,4'-Dithiobisbenzoic Acid (5)	14
1.3.4	Synthesis of Diphenyldisulfide (11)	15

1.3.5	Synthesis and Characterization of a Copper Complex with 4,4'-Dithiobisbenzoic Acid	15
-------	--	----

Chapter Two Development of Fluorinated and Imine-Based non-Covalent Organic Frameworks

2.1	Introduction to non-Covalent Organic Frameworks.....	18
2.2	Early Strategies in nCOF Construction	20
2.3	Results and Discussion.....	24
2.3.1	Partially Fluorinated Trigonal nCOF Precursors	24
2.3.1.1	Preparation of Partially Fluorinated Trigonal nCOF Precursor.....	24
2.3.1.2	Crystal Analysis of Partially Fluorinated Trigonal nCOF Precursor	25
2.3.2	Linear Imine-based nCOF Precursor	28
2.3.2.1	Preparation of Linear Imine-based nCOF Precursor	28
2.3.2.2	Crystal Analysis of Linear Imine-based nCOF Precursor.....	29
2.4	Conclusion and Outlook.....	32
2.5	Experimental Section.....	32
2.5.1	General Methods	32

2.5.2	Synthesis of 2,3,5,6-Tetrafluorobiphenyl (24)	33
2.5.3	Synthesis of 1,3,5-Tris[(2,3,5,6-Tetrafluoro-4-Phenyl)-Phenyl]Benzene (21)	34
2.5.4	Synthesis of 1,4-Dicyano-2,3,5,6-Tetrafluorobenzene (30)	36
2.5.5	Synthesis of 2,3,5,6-Tetrafluoroterephthalaldehyde (26)	37
2.5.6	Synthesis of 3-Chloro-1H-Pyrazol-4-Amine (27)	38
2.5.7	Synthesis and Characterization of Fluorinated Trisphenyl nCOF	39
2.5.8	Synthesis and Characterization of Linear Imine-Based nCOF	41

Chapter Three Self-sorting of Complex Libraries during Kinetically Controlled Acylations

3.1	Introduction to Self-sorting	43
3.2	Results and Discussion	47
3.2.1	Selectivity Tests in [2×2] Self-sorting Systems	47
3.2.2	Optimization of Acylation Self-sorting Conditions	49
3.2.3	Substrate Reactivity Arrangement	51
3.2.3.1	Establishment of Nucleophiles Reactivity List	51
3.2.3.2	Establishment of Acyl Chlorides Reactivity List	53

3.2.4	Selectivity tests in [3×3] Self-sorting Systems.....	54
3.3	Conclusion and Outlook.....	55
3.4	Experimental Section.....	55
3.4.1	General Synthetic and Characterization Methods.....	55
3.4.2	Selected Self-Sorting Experimental Procedure of [2×2] Acylation Mixture.....	56
3.4.3	Other Selective Acylation Self-sorting in [2×2] Systems.....	57
3.4.4	Selected Self-sorting Experimental Procedure of [3×3] Acylation Mixture.....	61
3.4.5	Other Selective Acylation Self-sorting in [3×3] Systems.....	62
3.4.6	Synthesis of Individual Amides and Thioesters.....	64
3.4.6.1	General Procedure for Synthesis.....	64
3.4.6.2	Compound Characterization	66
3.4.7	Experimental Apparatus	72
	References.....	73

ABBREVIATIONS AND ACRONYMS

1D	one-dimensional
2D	two-dimensional
3D	three-dimensional
BDC	1,4-benzenedicarboxylate (terephthalate)
BET	Brunauer-Emmett-Teller
BOC	<i>tert</i> -butyloxycarbonyl
Bu	butyl
CIF	crystallographic information files
CFC	chlorofluorocarbon
COF	covalent organic framework
DABCO	1,4-diazabicyclo[2.2.2]octane
DCC	dynamic covalent chemistry
DCL	dynamic combinatorial library
DCM	dichloromethane
DEF	<i>N,N</i> -diethylformamide
DMA	<i>N,N</i> -dimethylacetamide

DMF	<i>N,N</i> -dimethylformamide
DMSO	dimethyl sulfoxide
DNA	deoxyribonucleic acid
DTBB	4,4'-dithiobisbenzoic acid
DTT	dithiothrietol
Et	ethyl
Et ₃ N	triethylamine
Et ₂ O	ether
EtOAc	ethyl acetate
EtOH	ethanol
FT-IR	Fourier-transform
Hex	hexane
HCFC	hydrochlorofluorocarbon
HOF	hydrogen-bonded organic framework
IR	infrared
ISC	intersystem crossing
Me	methyl
MeOH	methanol

MOF	metal-organic framework
MOFF	fluorinated metal-organic framework
nCOF	noncovalent organic framework
NMR	nuclear magnetic resonance
Ph	phenyl
Pr	propyl
(<i>i</i> -Pr) ₂ NH	diisopropylamine
SBU	secondary building unit
SOF	supramolecular organic framework
TBAF	tetrabutylammonium fluoride
<i>t</i> -Bu	<i>tert</i> -butyl
THF	tetrahydrofuran
TLC	thin layer chromatography
TMS	trimethylsilyl
UV	ultraviolet
ZIF	zeolitic imidazole framework

Chapter One

Attempts to Prepare Metal-Organic Frameworks Based on Thiolated Precursors

1.1 Introduction

1.1.1 Introduction to Metal Organic Frameworks (MOFs)

Metal organic frameworks, i.e., MOFs, are compounds consisting of metal ions coordinated to organic molecules to form “infinite” structures that can be porous. Their studies constitute an interdisciplinary field with its origins in inorganic and coordination chemistry that has expanded rapidly in the last two decades, and is now also attracting the interest of the chemical industry.¹ The term "MOF" was first created by the Yaghi research group in 1995 for a layered cobalt-benzenetricarboxylate framework that showed reversible sorption properties towards aromatic guest molecules.² Later on the interest in this field was kindled again by the structure of MOF-5,³ and HKUST-1 (Hong Kong University of Science and Technology) also called Cu-BTC,⁴ both created in 1999 (Figure 1.1). MOF-5 is composed of zinc(II) clusters with terephthalic acid dianion as the organic linker, while Cu-BTC is composed of copper(II) paddlewheel dimers linked by trimesic acid trianion. From then on, an explosion of research interest in these inorganic hybrid materials comes from their proven viability as platforms for numerous applications, including gas storage,⁵ and separations,⁶ heterogeneous catalysis,⁷ ion-exchange,⁸ and drug delivery.⁹

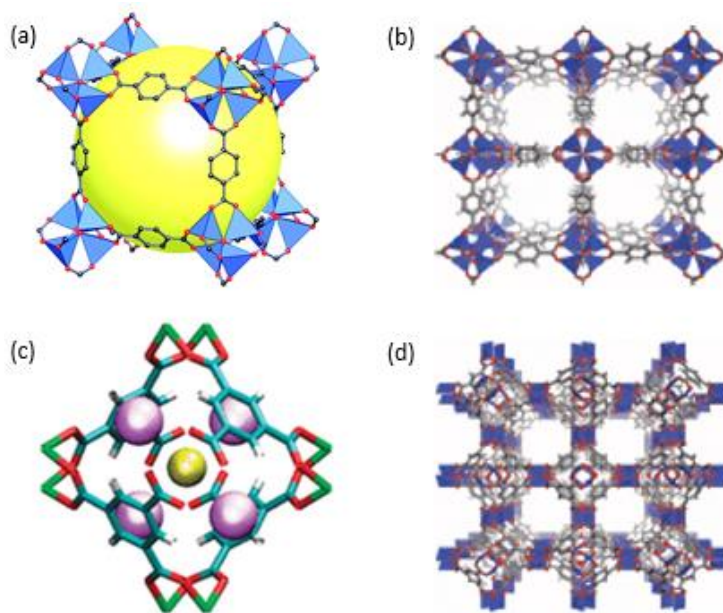


Figure 1.1 (a) Crystal structure of MOF-5. Oxygen and carbon are illustrated by red and black spheres respectively. Hydrogens are omitted. Secondary building units are presented as blue polyhedral. (b) Packing diagram of MOF-5 shows infinite three-dimensional network. (c) Crystal structure of Cu-BTC. Oxygen, carbon, and hydrogen atoms are illustrated in red, blue, and white, respectively. (d) Packing diagram of Cu-BTC shows infinite three-dimensional network.

In a typical synthesis of a MOF, the framework formation is templated by the SBU (secondary building unit) and the organic ligand, and are produced almost exclusively by hydrothermal or solvothermal techniques, where crystals slowly grow from a hot solution.¹⁰ Highly crystalline products can be analyzed with X-ray crystallography. The bulk materials can be investigated by powder X-ray diffraction (PXRD) analysis. The formation of a MOF crystal can be affected not only with the choice of starting materials and solvent, but also with external parameters, such as pH of

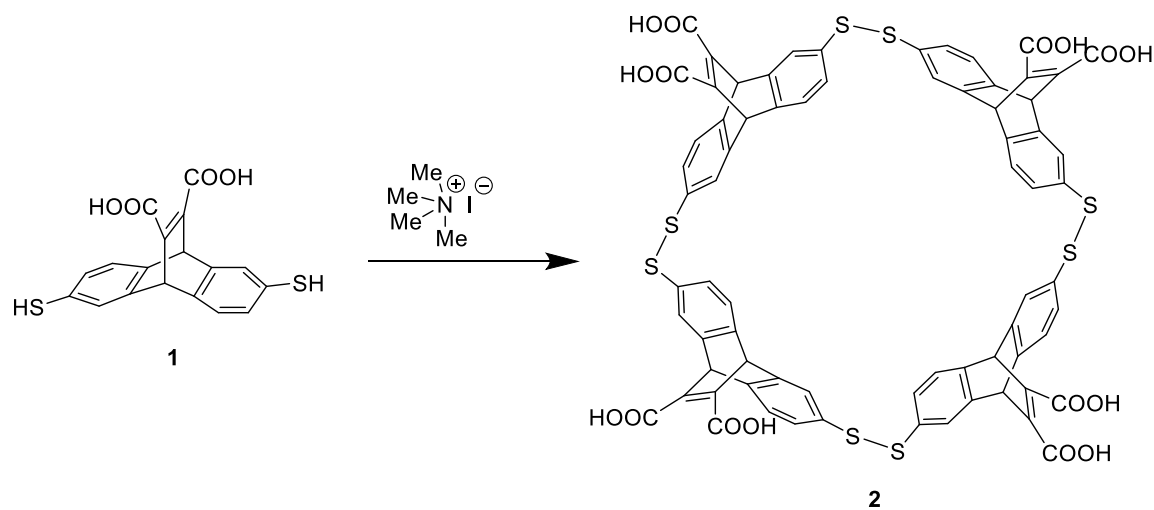
solution, reaction temperature, pressure, reaction time, cooling rate, etc. The self-assembly of metal ions, together with a variety of polyatomic organic bridging ligands, has resulted in tailored nanoporous host materials, which are robust solids with high thermal and mechanical stability.

Although the new strategies of designing and producing of new MOFs utilizing different ligands and metals are very successful, post-synthetic tailoring has also emerged as another robust strategy for integrating additional functionalities and properties into MOFs that could not be achieved during direct synthesis.¹¹ Examples of post-synthesis modification are to lengthen the ligand in order to further increase MOF's porosity,¹² and to cleave the protecting group so that non-interpenetrated versions of frameworks can be achieved.¹³ We were interested in the post-synthesis modification with a MOF crystal made from reversible ligand, and among all the potential reversible ligands, we chose to use the disulfide bond as it is often the "weak link" in many molecules and can be mildly reduced and reconnected.¹⁴

1.1.2 Introduction to Disulfide Exchange

Disulfide bonds are one of many dynamic covalent linkages employed in the creation of such thermodynamically controlled chemical systems. Two chemical reactions can be used to start the reaction: thiol oxidation, which generates a mixture of disulfides from thiols, and thiol-disulfide exchange, which allows a mixture of disulfides to exchange and reach equilibrium, so long as a catalytic amount of thiolate anion is

present. The disulfide chemical systems under rapidly attained thermodynamic equilibrium was developed independently by the research groups of Sanders.¹⁵ The thermodynamic outcome of covalently equilibrating systems affects the structure, constitution, and functionalities of the resulting product. Combinatorial chemistry under thermodynamic control leads to the generation of the so-called dynamic combinatorial libraries (DCLs) of interconverting species whose composition is adaptable and can be systematically altered by the application of environmental stimuli or chemical templates.¹⁶ For example, the racemic starting DCL of **1** can undergo exchange and self-assembly process to form tetramer **2**, in a process which is highly diastereoselective (Scheme 1.1).¹⁷



Scheme 1.1 Diastereoselective amplification of tetramer **2** from a DCL created from **1**.

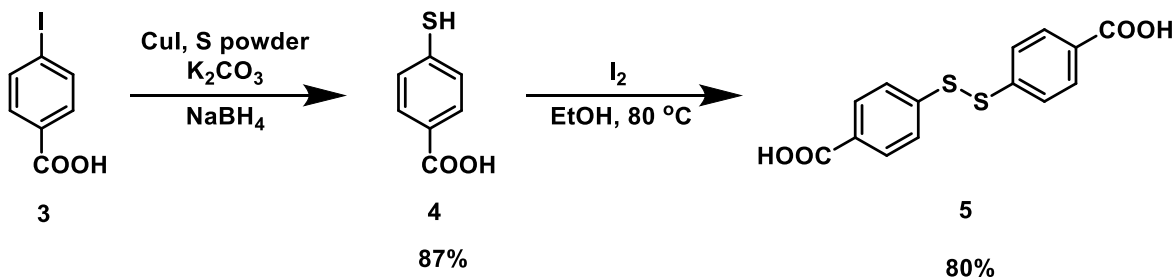
In the following section, our work on the synthesis and characterization of MOFs with reversibly formed disulfide linkages is described, including the attempted

recrystallization from the partially broken disulfide bonds and self-sorting among mixtures of different disulfide ligands.

1.2 Results and Discussion

1.2.1 Preparation of a MOF from 4,4'-Dithiobisbenzoic Acid

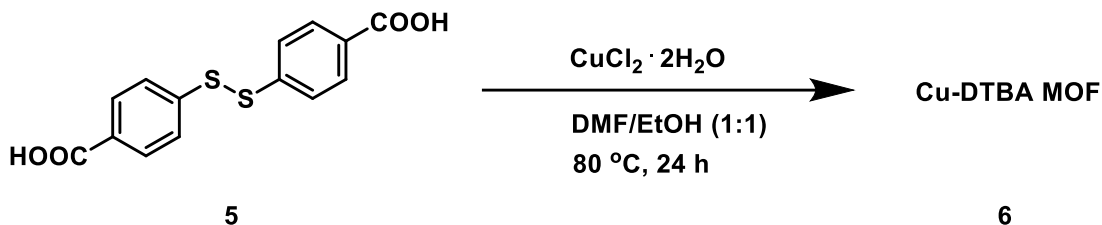
Ligand precursor—4,4'-dithiobisbenzoic acid **5** was synthesized according to the procedure shown in Scheme 1.2. Starting from 4-iodobenzoic acid **3**, sulfhydrylation with sulfur powder under basic condition affords 4-mercaptobenzoic acid **4**,¹⁸ which is oxidized by iodine in absolute ethanol to successfully afford 4,4'-dithiobisbenzoic acid **5** in 80% yield.¹⁹ This ligand precursor was used for the synthesis of copper-based MOFs described in the next subsection.



Scheme 1.2 Synthesis of disulfide-based ligand **5**.

To obtain our desired MOFs, a number of diverse reaction conditions were screened, with variable parameters that included temperature, reaction time, solvent composition, reactant ratio, and sometimes reaction vessel size. Finally, our first Cu-DTBA **5** (4,4'-dithiobisbenzoic acid) MOF was created through a solvothermal reaction, in which the mixture of **5** and 3 equivalents of CuCl₂·2H₂O was heated in a mixed solvent

system of DMF and EtOH (1:1) at 80 °C for 24 hours, producing the green cubic-shaped crystalline materials (Scheme 1.3).



Scheme 1.3 Synthesis of Cu-DTBA **6**.

Zn-based white crystals were also produced by treating **5** with $\text{Zn}(\text{NO}_3)_2 \cdot 6\text{H}_2\text{O}$, however, we were not able to get single crystal suitable for X-ray diffraction from these experiments.

1.2.2 X-ray Crystal Structure Analysis of Cu-DTBA MOF

To determine the structure of the obtained product, characterization of single crystal X-ray and PXRD were both conducted. The single-crystal X-ray structure of the new Cu-DTBA MOF **6** revealed a 1D structure with every ligand bent to an almost-perpendicular angle of 96.17° , measured by two centroids from the phenyl ring and one centroid from the middle of disulfide bond. Angle between two ligand is 90.51° , showed by two carbon atoms from two carboxylate groups and one centroid from the middle of Cu-Cu metal bond. Thus it formed a pseudo-rectangular unit cell (Figure 1.2). Each Cu(II) ion was coordinated with four oxygen atoms in four different bidentate carboxylate groups and one oxygen from monodentate solvent molecules.

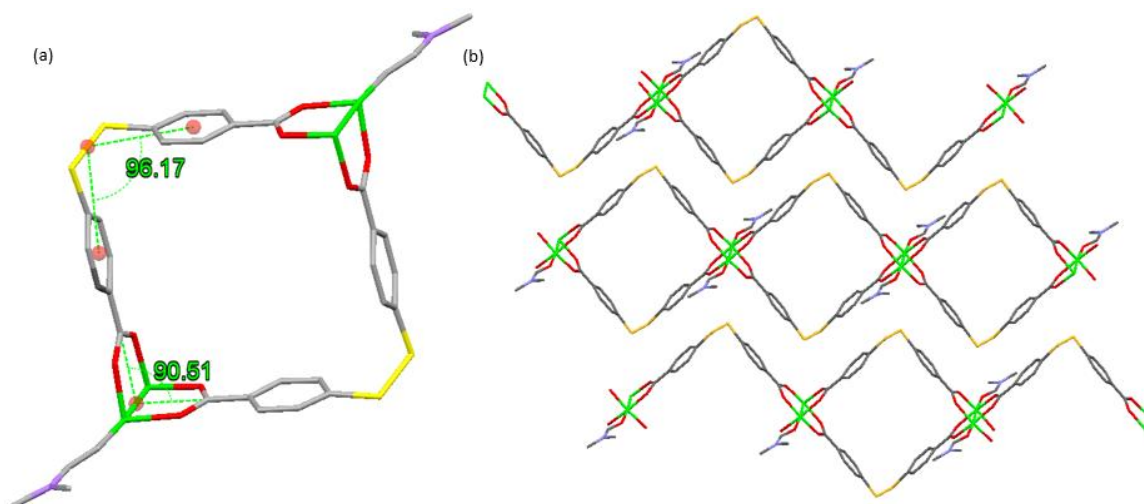


Figure 1.2 (a) Unit cell of Cu-DTBA crystal. Oxygen, sulfur, and carbon atoms are illustrated in red, yellow, and black, respectively. Hydrogen atoms omitted for clarity. (b) Packing diagram of three parallel 1D chains.

The right-angle dicarboxylate acid ligand directs the reticulation of the paddle wheel cluster. Two carboxylic group protons in each acid molecule were deprotonated by the base that was formed by high-temperature decomposition of *N,N'*-dimethylformamide (DMF), and thus these carboxylate anions were connected to Cu center forming tetrahedral secondary building unit (SBU), which then propagates into “infinite” 1D architecture. Two types of 1D chains are packed in the different layer, one in horizontal position while the other in diagonal position (Figure 1.3), resulting in monoclinic crystalline structure (Table 1.1). Every 1D chain is isolated in the structure.

Table 1.1 Crystallographic data for **6**.

Compound name	
Chemical formula	$\text{C}_{14}\text{H}_8\text{CuN}_{0.13}\text{O}_4\text{S}_2$
Formula Mass	369.62
Crystal system	Monoclinic
$a/\text{\AA}$	17.408(2)
$b/\text{\AA}$	13.3308(15)
$c/\text{\AA}$	18.806(3)
$\alpha/^\circ$	90.00
$\beta/^\circ$	106.445(11)
$\gamma/^\circ$	90.00
Unit cell volume/ \AA^3	4185.6(10)
Temperature/K	223(2)
No. of formula units per unit cell, Z	8
Radiation type	MoK α
Absorption coefficient, μ/mm^{-1}	1.250
No. of reflections measured	4804
No. of independent reflections	2577
R_{int}	0.1407
$R_1 (I > 2\sigma(I))$	0.0770
$wR(F^2) (I > 2\sigma(I))$	0.1990
R_1 (all data)	0.1562
$wR(F^2)$ (all data)	0.2554
Goodness of fit on F^2	0.930

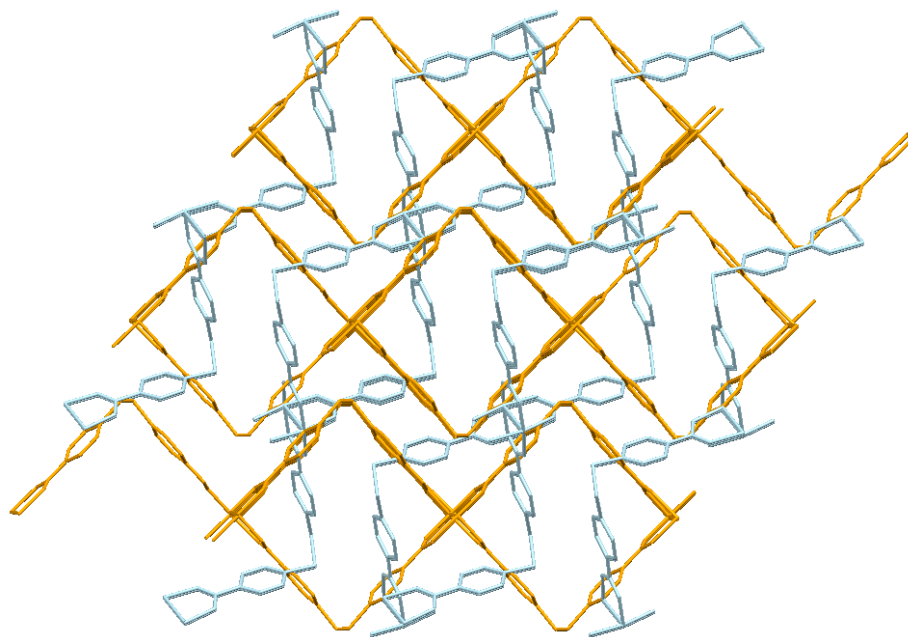


Figure 1.3 Packing diagram of two types of chain structure, orange chain (from left to right) is located in the horizontal position, while blue chain is located in diagonal position. Solvent molecules are omitted for clarity.

1.2.3 Attempted Reduction and Recrystallization of Cu-DTBA MOF Crystals

The organizing motif of our new MOF was capped paddlewheel binuclear Cu cluster, in which two Cu ions are bridged by four carboxylic groups into a paddlewheel geometry, and then connected with two solvent molecules of H₂O. Therefore, since the structure of **6** had the S–S bridge between two secondary building units, we hoped to see that readily reducible disulfide bond cut off, while maintaining the structure of secondary building units. Thus, we treated our Cu-DTBA MOF crystal **6** with a mild reductive reagent dithiothriitol (DTT) **7** in a wide range from 1 to 50 equivalents, in different

solvents. We expected to see the disulfide exchange, that is, initial ionization of the DTT to thiolate anion, followed by nucleophilic attack on the sulfur atom of the crystal linkage disulfide moiety to cleave the original S–S bridge and form the six-member ring **10** (Figure 1.4).²⁰ Unfortunately, this reaction failed. After 3 days, the green crystals gradually turned to a yellow precipitate. We filtered out this precipitate in the solution and washed it with MeOH, but we couldn't get our green crystals back when put them back into a new vial and apply the original crystallization condition. Later the ¹H NMR spectrum was also checked, and it only showed the existence of 4-mercaptobenzoic acid without any other species.

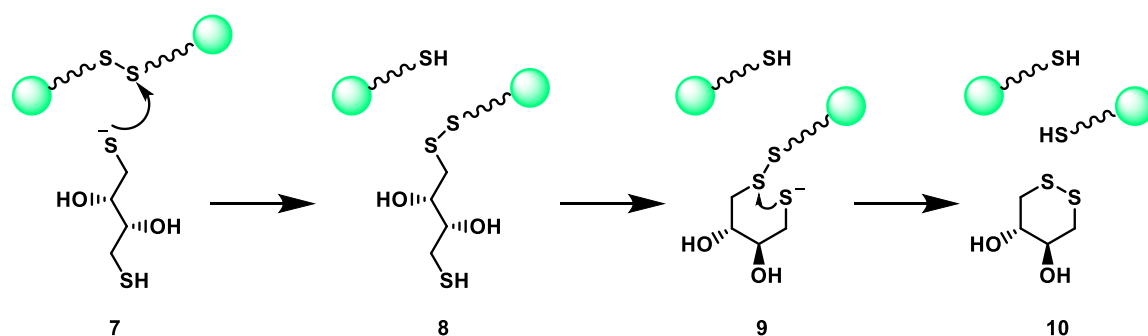


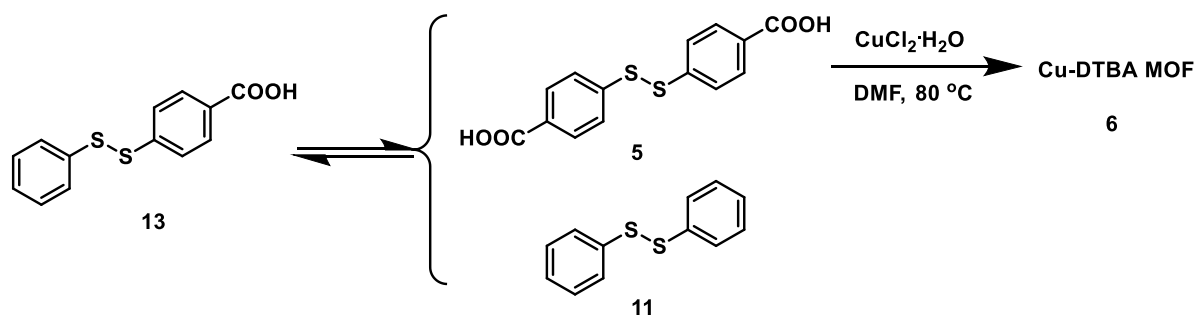
Figure 1.4 Reduction of the disulfide bond by DTT **7** via two sequential thiol-disulfide exchange reactions.

To conclude the failure of this experiment, the Cu–O coordination bond may not be strong enough when facing the interference of other coordinators. In addition to this, the framework was not very rigid because of formation via relatively flexible disulfide ligand, making it more difficult to reproduce.

1.2.4 Copper-Catalyzed Self-Sorting between Disulfide Ligands

In general, Cu is a soft late transition metal which prefers to bond to other soft and polarizable atoms like S. Therefore, the coordination system between Cu and O should be in an equilibrium. The diphenyldisulfide **11** was readily formed by oxidation of mercaptobenzene **12** in hot DMSO. We applied our original condition from Cu–DTBA MOF again to this mixture, and we were able to get the same green crystals **6**. In fact, PXRD pattern shows the crystal produced from the mixture exactly matched with our original Cu–DTBA MOF crystals **6**.

Encouraged by the intermolecular self-sorting success, we decided to have a try on its intramolecular self-sorting ability. We planned to make the pure cross-ligand **13** and expected the crystallization of copper with the cross-ligand to result in self-sorting into two pieces: 4,4'-dithiobisbenzoic acid **5** and diphenyldisulfide **11** (Scheme 1.4). Indeed, the ligand **13** was made before by mixing 4,4'-dithiobisbenzoic acid **5** and diphenyldisulfide **11** with 1:1 ratio in the DMF under 80 °C and followed by column chromatography. The purity of ligand was confirmed by HPLC.



Scheme 1.4 Retro synthesis of pure cross-linked ligand **13** from **5** and **11** and Copper-mediated atalyzed self-sorting from compound **13**.

However, the second experiment's PXRD spectrum from the cross-ligand **13** looks very different from the original one. The crystals in second experiment were much smaller. We also tried to get the single crystal from the cross-ligand by varying the conditions, but we never succeeded in that.

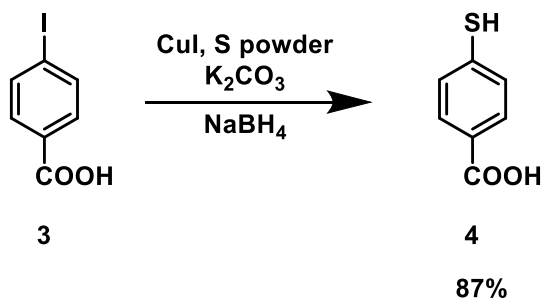
1.3 Experimental Section

1.3.1 General Procedures

All reagents and solvents were obtained from commercial suppliers and used without further purification. Solvents were used as received, except acetonitrile (MeCN), which was dried over activated alumina in an mBraun Solvent Purification System. Triethylamine (Et_3N) and diisopropylamine ($i\text{-Pr}_2\text{NH}$) were used after distillation over KOH pellets and 20-minute degassing with nitrogen purge. Column chromatography was carried out on silica-gel 60, 32–63 mesh. Analytical TLC was performed on JT Baker plastic-backed silica gel plates. ^1H NMR spectra were recorded on JEOL ECX-400 and

ECA-500 spectrometers, with working frequencies (for ^1H nuclei) of 400 and 500 MHz, respectively. ^1H NMR chemical shifts are reported in ppm units relative to the residual signal of the solvent (CDCl_3 : 7.26 ppm, $\text{DMSO}-d_6$: 2.50 ppm), and multiplicity is expressed as follows: s = singlet, d = doublet, m = multiplet. All NMR spectra were recorded at 25 $^\circ\text{C}$. Single crystal X-ray diffraction measurements were performed at the Texas State University–San Marcos X-ray laboratory, using a Rigaku SCX-Mini diffractometer, equipped with a Mo tube and SHINE optics. Crystals were mounted on a glass fiber for measurement. Data collection and data integration were completed using Process-Auto. Solutions were generated by direct methods using SHELXS-97.

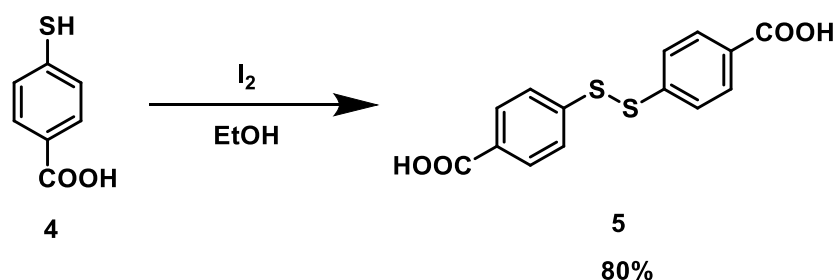
1.3.2 Synthesis of 4-Mercaptobenzoic Acid (**4**)



An oven-dried Schlenk tube was charged with CuI (95 mg, 0.50 mmol), 4-iodobenzoic acid **3** (1.24 g, 5.00 mmol), S powder (480 mg, 15.0 mmol), and K₂CO₃ (1.38 g, 10.0 mmol). The tube was evacuated and backfilled with nitrogen before DMF (10 mL) was added. The reaction mixture was stirred at 90 $^\circ\text{C}$ until the 4-iodobenzoic acid **3** was completely consumed as monitored by TLC. To this reaction mixture, NaBH₄ (0.55 g, 15.0 mmol) was added with cooling by ice-water. After the resultant reaction

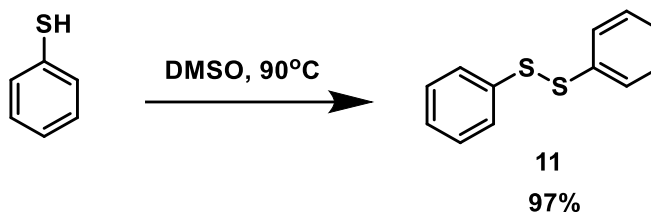
solution was stirred at 40 °C for 5 h, 3 N HCl (10 mL) was added to quench the reaction. The mixture was extracted with EtOAc, and the combined organic layers were treated with 20% NaOH. The aqueous layer was separated, washed with EtOAc, acidified with concentrated HCl, and then extracted with EtOAc. The organic layer was washed with H₂O and brine, and dried over Na₂SO₄. Removal of solvent in *vacuo* provided the desired product with 87% yield. Spectral data agree with literature report.²¹

1.3.3 Synthesis of 4,4'-Dithiobisbenzoic Acid (5)



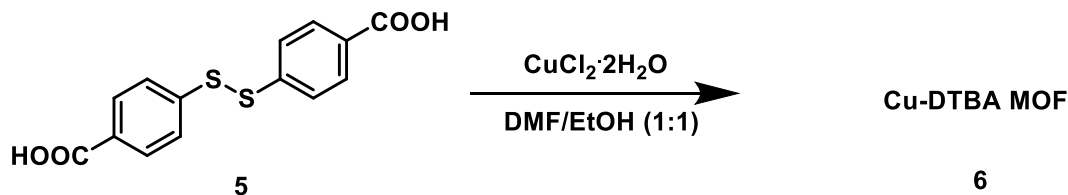
This procedure is a modified version of the procedure described by Evans for the preparation of aromatic disulfides.²² 4-Mercaptobenzoic acid **4** (0.53 g, 3.40 mmol) and iodine (0.44 g, 1.70 mmol) were dissolved in 10 mL of absolute EtOH. Triethylamine (1.5 mL) was added and the solution was stirred for 16 h. Excess iodine was removed by reduction with 10% sodium thiosulfate solution. The cloudy solution was concentrated and combined with 60 mL of 0.01 M hydrochloric acid. The white precipitate was collected and dried under vacuum. The product was recrystallized from *N,N*-dimethylacetamide (DMA) and water (0.51 g, 80% yield). Spectral data agree with a previous literature report.²²

1.3.4 Synthesis of Diphenyldisulfide (11)



An equimolar mixture of thiophenol (1.57 mL, 15.3 mmol) and DMSO (0.90 mL, 15.3 mmol) was heated at 90 °C for 4 h. The reaction mixture was cooled to room temperature, diethyl ether was added and washed with water. The organic phase was dried over anhydrous magnesium sulfate and evaporated to dryness in *vacuo* to give product. This compound was obtained as a white crystalline solid in a 97% yield (1.63 g, 14.9 mmol). Spectral data agree with literature report.²³

1.3.5 Synthesis and Characterization of a Copper Complex with 4,4'-Dithiobisbenzoic Acid



Ligand 4,4'-dithiobisbenzoic acid (20 mg, 0.039 mmol) and metal $\text{CuCl}_2 \cdot 2\text{H}_2\text{O}$ were mixed in 1.5 mL mixed solvent of DMF and EtOH (1:1) in ten 4 mL vials. The vials were sealed with Teflon tape, capped firmly, and then heated in an oven at 80 °C for 24 h. The vials were removed and slowly cooled to room temperature. The solvent was removed, and resulting crystalline materials were washed several times with fresh DMF

and then MeOH. Most vials produced green cubic-shaped crystals, which were characterized with single crystal X-ray crystallography.

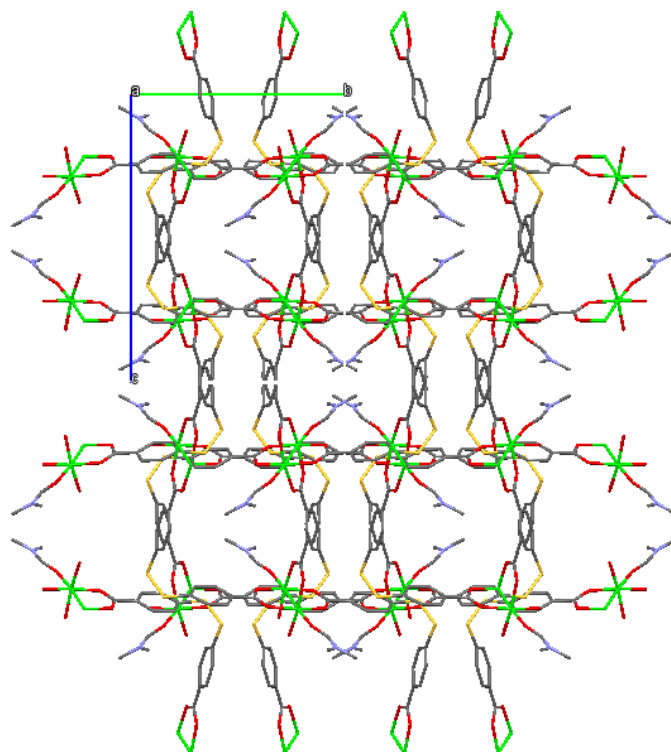


Figure 1.5 1D network of Cu-DTBA MOF along the crystallographic a axis. The gray, red, white, yellow, and green colors represent the carbon, oxygen, hydrogen, sulfur, and copper atoms, respectively.

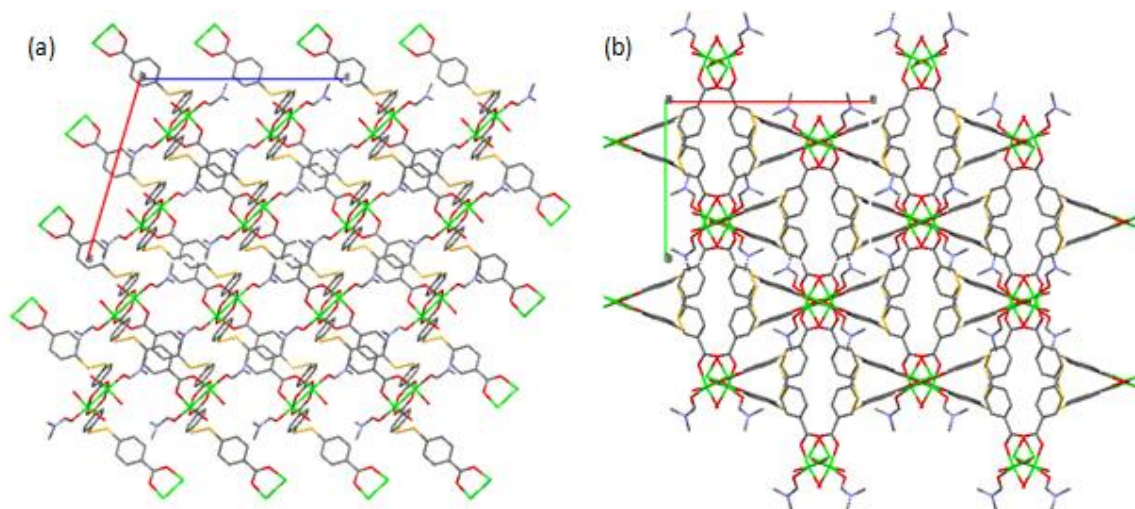


Figure 1.6 (a) 1D network of Cu-DTBA MOF along the crystallographic b axis. (b) 1D network of Cu-DTBA MOF along the crystallographic c axis. The gray, red, white, yellow, and green colors represent the carbon, oxygen, hydrogen, sulfur, and copper atoms, respectively.

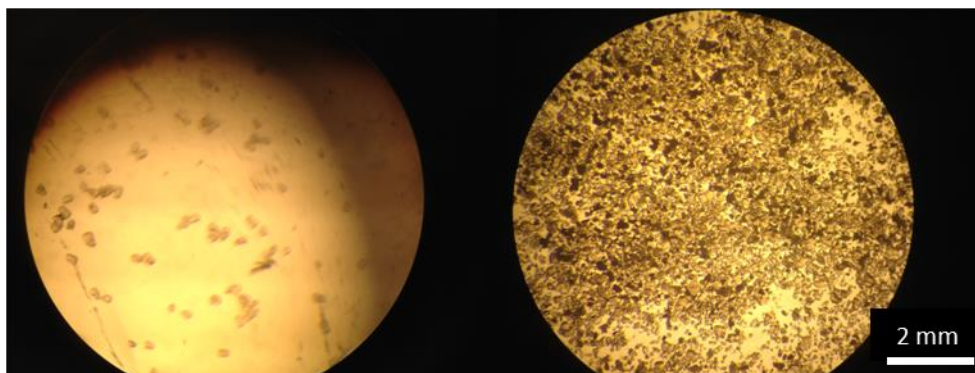


Figure 1.7 Microscopy image of crystal **6**, revealing cubic morphology.

Chapter Two

Development of Fluorinated and Imine-Based non-Covalent Organic Frameworks

2.1 Introduction to non-Covalent Organic Frameworks

Porous solids are of scientific and technological interest because of their ability to interact with atoms, ions and molecules not only at their surfaces, but throughout the internal structure of the material. The past decade has seen significant advances in the ability to fabricate new porous solids with ordered structures from a wide range of different materials.²⁴ Most crystalline porous materials with permanent pores are extended structures composed of directional covalent or coordination bonds, such as metal organic (MOFs) and covalent organic frameworks (COFs), and organic network polymers. In contrast, non-covalent organic frameworks (nCOFs) crystals are composed of discrete molecules between which there are only hydrogen bonds and other non-covalent interactions—i.e., π - π stacking, hydrophobic interactions, etc., are the rarest members of the porous materials family.²⁵ Among porous materials, non-covalent organic frameworks (nCOFs), which possess lower densities than other porous materials have attracted much research interest in recent years.²⁶

nCOFs were proposed as potential porous materials with most likely applications being in gas storage, separation, sensing, and catalysis.²⁷ They are expected to have not only the advantages such as high thermal stabilities, easy purification, and solution characterization, but also some very useful and unusual properties; lower densities and

better gas separation than other porous materials, due to the more flexible structure; as well as easy regeneration through simple recrystallization.²⁸

The development of nCOFs has lagged significantly behind other porous organic materials. The first example of nCOF was published in 1991 by Wuest and his coworkers based on the principles of molecular tectonics—a tetrahedral molecule, containing four pyridone “sticky sites” **14** was found to assemble into a diamondoid crystal structure, which could subsequently be desolvated to generate a permanently porous structure (Figure 2.1).²⁷ Since then, the research in this field progressed slowly, until the rapid evolution from around 2009.²⁹ In fact, within these two decades, thousands of non-covalent organic structures have been produced. But most of these structures usually collapse after removal of the guest molecules due to the relatively weak interactions among the ligands, and consequently are not likely to be useful.³⁰ However, a few nCOFs exhibit permanent porosity even after heating, and these crystals often have a large amount of hydrogen bonding and π - π stacking, the collective effect of which is to help protect the crystal structure against collapse.³¹

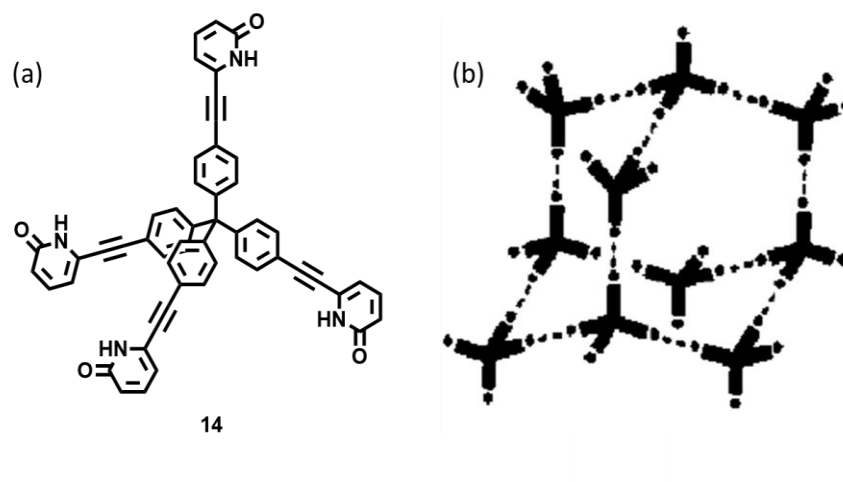


Figure 2.1 (a) Tetrahedral molecular structure of **14**; (b) schematic representation of the crystal structure formed with **14**.

2.2 Early Strategies in nCOF Construction

Two main strategies so far have been used to prepare porous organic molecular solids, intrinsically and extrinsically. Macrocycles³² and molecular cages³³ with pores, which are synthetically prefabricated in the molecules and can be identified by viewing the structure of an isolated molecule, are intrinsically porous. Metal organic polyhedra³⁴ and heme-like coordination crystals³⁵ also exhibit intrinsic porosity of this type. Crystallization of these molecules will still keep their intrinsic pores while forming an ordered extended structure. For example, the macrocycle-based porous organic solid **16** is assembled from [6+2] supramolecular units composed of six calix[4]-dihydroquinone **15** and two water molecules (Figure 2.2).

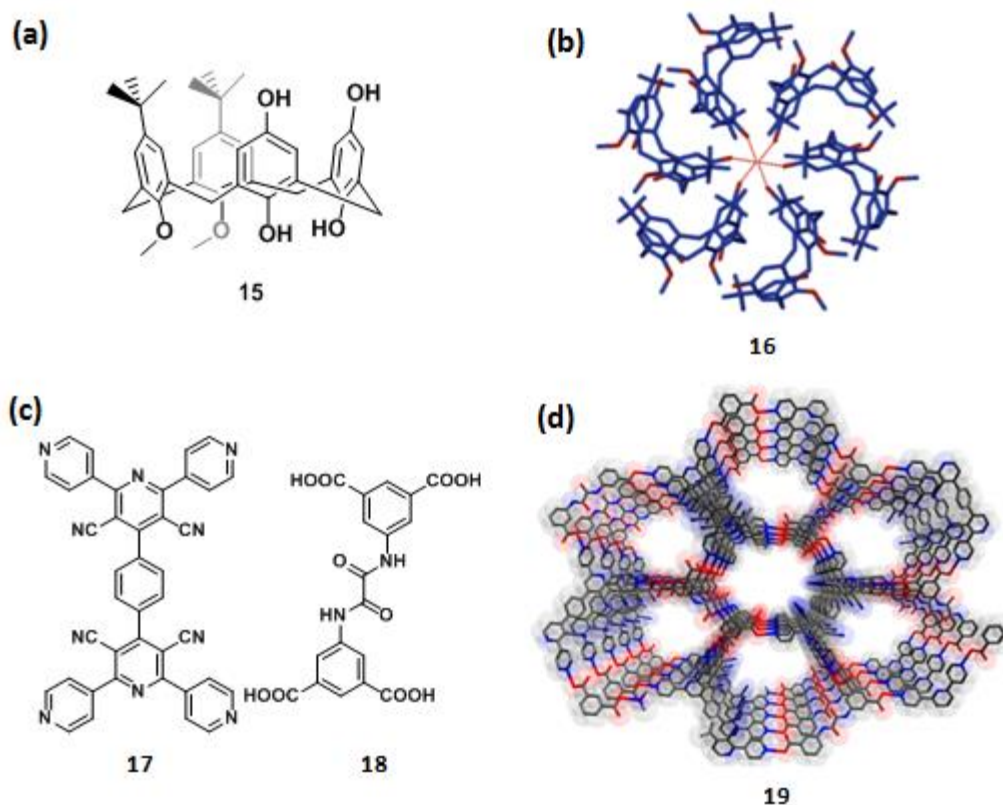


Figure 2.2 (a) Molecular structure for macrocycle **15**; (b) supramolecular network of **16**, six calixarenes and two water molecules are connected by hydrogen bonding showing in red dotted line; (c) Molecular structure of both **17** and **18**. (d) infinite 3D network with two types of 1D channels. Oxygen and nitrogen atoms are colored in red and blue.

This nCOF shows a remarkable CO₂ absorption due to the hydrophobic cavities. Other systems have extrinsic porosity and the pore structure arises purely from the molecular packing. For instance, a robust binary SOF-7 (**19**), made of organic building blocks **17** and **18** via solely hydrogen bonding, features a 3D, four-fold interpenetrating lattice containing channels decorated with cyano and amido groups.³⁶ This extrinsically permanent porosity gives it excellent CO₂ adsorption capacity and selectivity over C₂H₄.

In general, extrinsic porosity may not be obvious from inspection of the isolated molecular structure. However, these materials usually pack in high order so that it generates channels which made them porous.

Our group has also succeeded in synthesis and characterization of a novel type of trispyrazole ligand **20** that organizes into a robust, extrinsically porous non-covalent organic framework (Figure 2.3). Considering that solid-state fluorinated porous materials can be useful for storage and capture of fluorinated compounds such as chlorofluorocarbons (CFCs, also known as Freons), we applied the function of fluorination into this new type of nCOF's synthesis.³⁷ The new fluorinated trispyrazole ligand **20** formed a three-dimensional network results, with infinite one-dimensional channels protruding throughout the crystal along the crystallographic *c* axis. The combination of hydrogen bonding and π - π stacking contributed to the network construction.

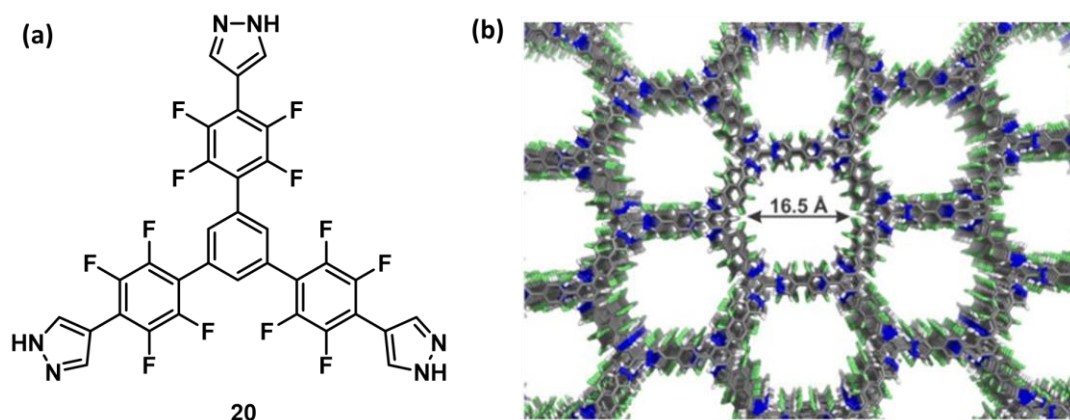


Figure 2.3 (a) Molecular structure of compound **20**. (b) 3D hexagonal network with infinite fluorine-lined channels protruding throughout the structure along the crystallographic *c*-axis.

This new material is lightweight, thermally and hydrolytically stable and is a superb adsorbent for hydrocarbons and their halogenated derivatives, many of which are potent greenhouse gases. Its porosity and gas binding ability rank highly among the other non-covalently connected materials presented to date. But its synthesis and structural characterization also raised several questions. Can pyrazole be replaced with other functionalities that could allow the dissection and fine tuning of hydrogen bonding and π - π stacking effects? Can this porosity and selective absorbing ability be reached by a linear fluorinated ligand?

In this chapter, to answer the two questions above, we present the synthesis and characterization of a new fluorinated nCOF precursor, in which pyrazoles are switched to phenyl rings, as well as a fluorinated linear imine-based nCOF instead of the previous trigonal shape. Both of them formed closely-packed nCOF crystals. The former nCOF

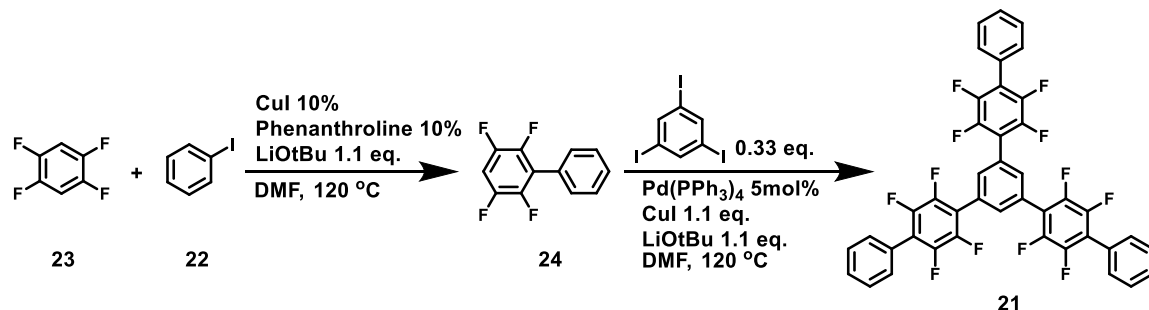
only shows π - π interactions between its constituent units, while the latter one has both π - π stacking and hydrogen bonding.

2.3 Results and Discussion

2.3.1 Partially Fluorinated Trisphenyl nCOF

2.3.1.1 Preparation of Partially Fluorinated Trisphenyl nCOF

Fluorinated trisphenyl ligand **21** was synthesized in two steps from the commercially available iodobenzene **22**, which was subjected to a Cu-catalyzed coupling with an excess of 1,2,4,5-tetrafluorobenzene **23** to produce intermediate **24** (Scheme 2.1). Thus, only one of the two C-H bonds of tetrafluorobenzene was replaced with a phenyl ring moiety. Next, another Pd-catalyzed coupling followed, combining 3.3 equivalents of 2,3,5,6-tetrafluoro-1,1'-biphenyl with 1,3,5-triiodobenzene and resulting in the trigonal precursor. In each arm there is an electron-rich ring on the end as well as an electron-poor fluorinated ring in the middle. This trigonal fluorinated ligand was then used for the synthesis of framework.



Scheme 2.1 Synthesis process of the partially fluorinated trisphenyl compound **21**.

Because compound **21** is much more soluble in most solvents than the original trispyrazole ligand **20**, it does not need extra Boc-protecting groups to help with solubility at all. Thus, we tried to grow crystals using both solvent diffusion and slow evaporation methods. The latter method was more successful, allowing us to produce high quality single crystals after two days evaporation of the THF solution of **21**.

2.3.1.2 Crystal Analysis of Partially Fluorinated Trisphenyl nCOF

This white transparent crystal came out of the solution in hexagonal shape. From the single crystal structure, it revealed a zigzag structure, which was classified as orthorhombic crystal system with space group *Pbcn* (Table 2.1). In the molecular structure, the dihedral angles between the adjacent planes of terminal phenyl ring and tetrafluorobenzene ring are different, ranging from 43.92° to 55.53°. Two phenyl rings out of three are nearly parallel to the central phenyl ring, while the other one is about 7° off. This resulted in different functions in three arms. The top two provide the electron rich phenyl rings (red) to establish the short contacts, π - π interactions, while the bottom arm provides the electron-poor tetrafluorobenzene ring (Figure 2.4).

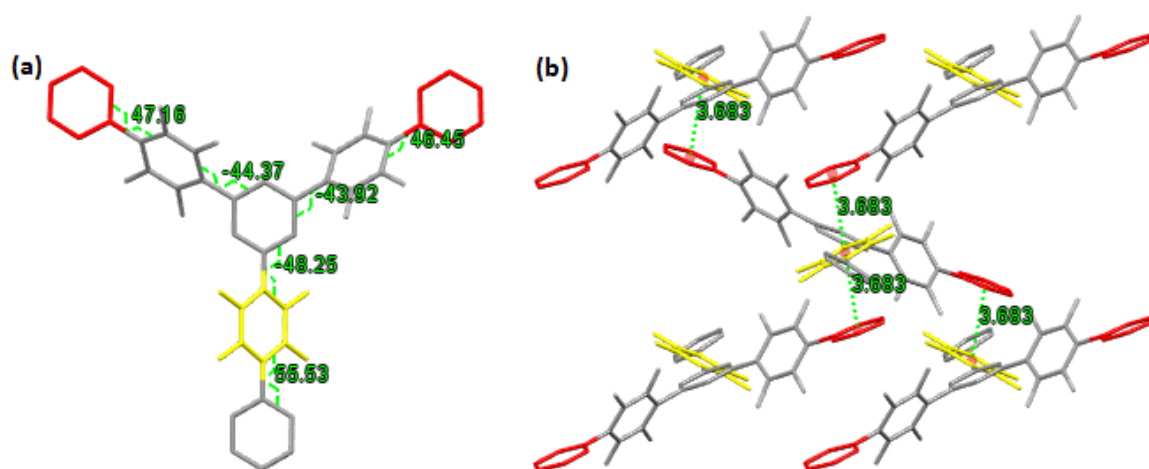


Figure 2.4 (a) Dihedral angles in the molecule showed three arms are not symmetrical, ones parallel to the central ring are able to build up π - π interactions; (b) π - π stacking between terminal phenyl rings (red) and 1,2,4,5-tetrafluorobenzene rings (yellow).

The distance between the electron-rich benzene rings and electron-poor 1,2,4,5-tetrafluorobenzene rings are 3.68 Å. (Centroid-centroid distances are quoted because ring planes are not parallel and thus interplanar distance cannot be determined). Each molecule has four π - π interactions from the tetrafluorobenzene ring covered by two neighbor molecules, and another two from the terminal phenyl rings. Thus, the molecules were lined up in a three-dimensional crystal structure. However, molecules of **21** closely pack, and do not have significant voids inside, resulting in a non-porous nCOF crystal.

Table 2.1 Crystallographic data for the fluorinated trisphenyl nCOF.

Compound name	
Chemical formula	C ₄₂ H ₁₈ F ₁₂
Formula Mass	750.56
Crystal system	Orthorhombic
<i>a</i> /Å	13.1526(2)
<i>b</i> /Å	19.5199(3)
<i>c</i> /Å	12.3721(2)
α /°	90.00
β /°	90.00
γ /°	90.00
Unit cell volume/Å ³	3176.38(9)
Temperature/K	123(2)
Space group	Pbcn
No. of formula units per unit cell, Z	4
Radiation type	CuK α
Absorption coefficient, μ /mm ⁻¹	1.230
No. of reflections measured	3150
No. of independent reflections	2730
<i>R</i> _{int}	0.0187
<i>R</i> ₁ (<i>I</i> > 2 σ (<i>I</i>))	0.0334
<i>wR</i> (<i>F</i> ²) (<i>I</i> > 2 σ (<i>I</i>))	0.0947
<i>R</i> ₁ (<i>all data</i>)	0.0341
<i>wR</i> (<i>F</i> ²) (<i>all data</i>)	0.0956
<i>Goodness of fit on F</i> ²	1.085

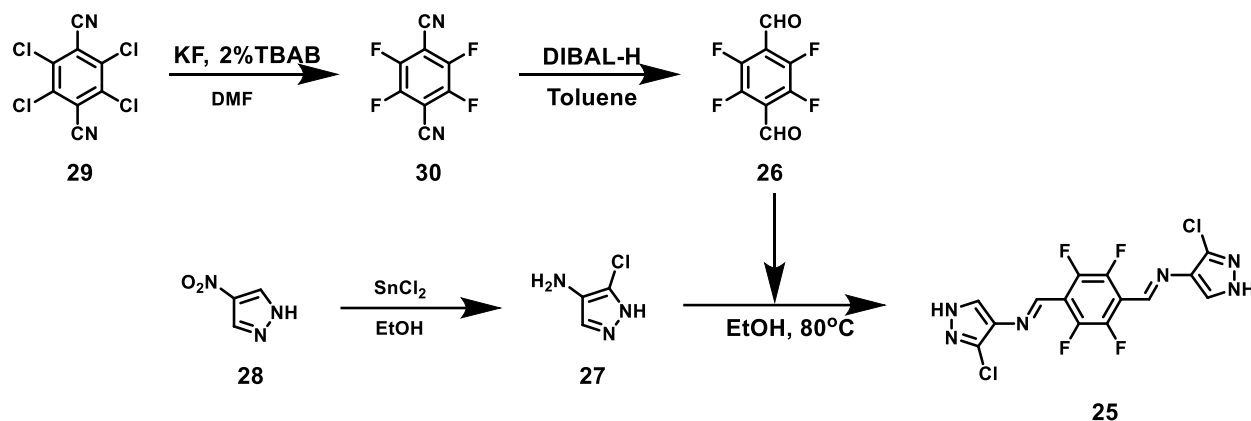
This somewhat disappointing result seems to suggest that both π - π stacking and hydrogen bonding are essential for the assembly of robust porous structures from small trigonal precursors. Our next challenge was to determine whether trigonal structure is

also essential for the creation of a porous crystal; to probe this, we have prepared a fluorinated linear imine-based nCOF.

2.3.2 Linear Imine-based nCOF

2.3.2.1 Preparation of Linear Imine-based nCOF

This linear imine-based ligand **25** was designed from three substrate building blocks, one dialdehyde molecule **26** as well as two chloroamino pyrazole molecules **27** (Scheme 2.2). Our initial target was to make aminopyrazole. We treated starting material nitro-pyrazole **28** with the reducing reagent SnCl_2 in EtOH, expecting to get amino-pyrazole synthesized partially following the procedure from our group's previous publication.³⁸ However, after full characterization of the product, we found not only that the nitro group was reduced, but also one proton on the pyrazole ring was substituted by chlorine. Therefore, we obtained 3-chloro-1H-pyrazol-4-amine **27**. On the other hand, our approach to 1,2,4,5-tetrafluoroterephthaldehyde (**26**) utilized commercially available 2,3,5,6-tetrachloro-1,4-dicyanobenzene **29** as the starting material. Tetrafluorocyano compound **30** was prepared in 89% yield by facile Cl/F exchange using KF in DMF along with 2% phase transfer agent tetrabutyl ammonium bromide. The cyano groups were then reduced using DIBAL-H in toluene to form compound **27**.



Scheme 2.2 Synthesis of the partially fluorinated linear imine-based nCOF.

We then treated our compound **26** with two equivalents of compound **27**, and applied the normal imine formation condition in EtOH under 80 °C for 12 hours. Finally, we obtained yellow crystals as expected.

2.3.2.2 Crystal Analysis of Linear Imine-based nCOF

Single-crystal X-ray diffraction structure of the linear imine-based nCOF showed that the crystal system was monoclinic (Table 2.2). In the unit cell, the two pyrazole rings are located both above and below the middle tetrafluorobenzene ring, and all three rings are parallel to each other (Figure 2.5). From the crystal structure, each molecule is two thirds sandwiched by two closest neighbors through π - π interactions, formed between electron-rich pyrazole ring and electron-poor tetrafluorobenzene ring; two from top and another two from bottom. The centroid-centroid distances of every pyrazole ring and tetrafluorobenzene ring pair are within 3.783 Å. Centroid-centroid distances are quoted because ring planes are not parallel and thus interplanar distance cannot be determined. This π - π stacking creates 1D chains along *c*-axis. In the meantime, chlorinated pyrazoles

at the end of each molecule establish hydrogen bonding with two adjacent molecules. These N \cdots H bonding distances are 2.384 Å, and four hydrogen bondings are formed from one molecule which is located in the middle among the four nearest neighbors. This also makes the whole structure reach the best space filling and therefore produce the lowest entropy. Overall, these hydrogen bonds connect all of 1D chains which build up by π - π stacking and finally create a three-dimensional network.

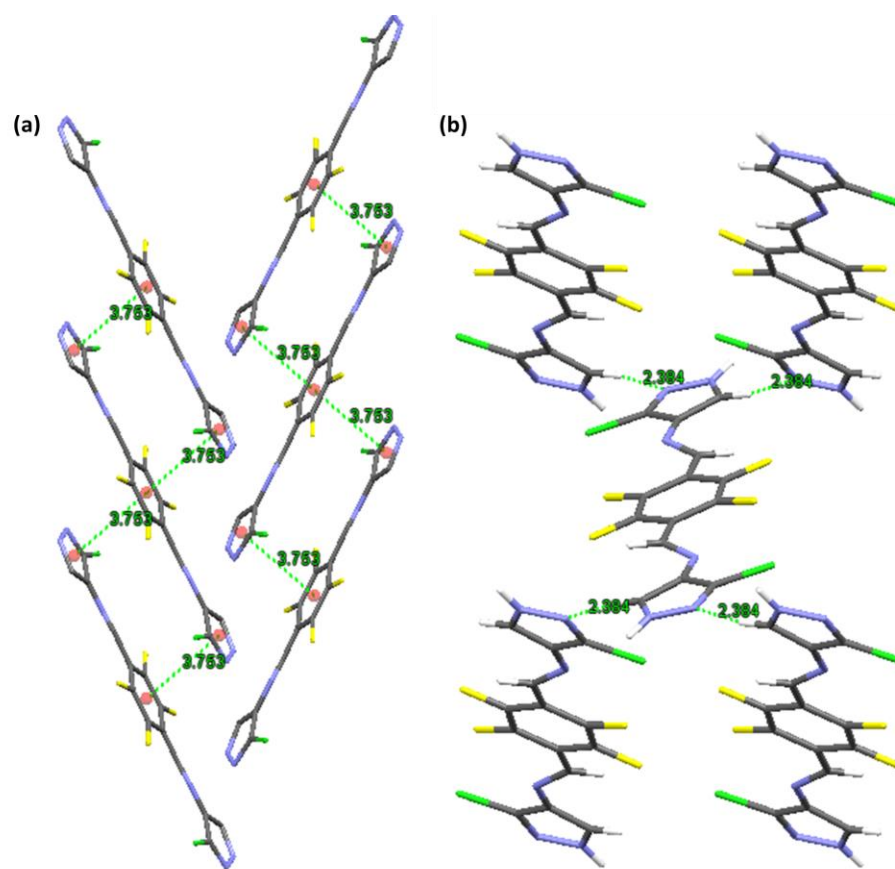


Figure 2.5 (a) π - π stacking between pyrazole rings and tetrafluorobenzene rings, measured by centroid-centroid distance; (b) hydrogen bonding established from each pyrazole to its two neighbors. The gray, purple, yellow, white and green colors represent the carbon, nitrogen, fluorine, hydrogen and chlorine atoms, respectively.

Table 2.2 Crystallographic data for the partially fluorinated linear imine-based nCOF.

Compound name	
Chemical formula	C ₁₄ H ₆ Cl ₂ F ₄ N ₆
Formula Mass	405.15
Crystal system	Monoclinic
<i>a</i> /Å	7.2212(4)
<i>b</i> /Å	12.9730(6)
<i>c</i> /Å	8.0959(4)
α /°	90.00
β /°	90.812(2)
γ /°	90.00
Unit cell volume/Å ³	758.35(7)
Temperature/K	213(2)
Space group	P2(1)/n
No. of formula units per unit cell, Z	4
Radiation type	CuK α
Absorption coefficient, μ /mm ⁻¹	4.423
No. of reflections measured	1361
No. of independent reflections	1268
<i>R</i> _{int}	0.0241
<i>R</i> ₁ (<i>I</i> > 2 σ (<i>I</i>))	0.0306
<i>wR</i> (<i>F</i> ²) (<i>I</i> > 2 σ (<i>I</i>))	0.0860
<i>R</i> ₁ (<i>all data</i>)	0.0311
<i>wR</i> (<i>F</i> ²) (<i>all data</i>)	0.0866
<i>Goodness of fit on F</i> ²	1.064

To our disappointment, this closely packed structure was not porous either. In the future, trigonal ligands should be the target while applying *in situ* imine formation strategy to make new nCOFs.

2.4 Conclusion and Outlook

Because nCOFs have many advantages, such as solution processability and characterization, easy purification, and straightforward regeneration by simple recrystallization over porous MOF materials, some porous nCOF materials might be potentially implemented in industrial and/or pharmaceutical applications. Thus, further research endeavors should target on understanding of the basic and strong hydrogen-bonding motifs to stabilize the frameworks, rationalizing that the basic principles for constructing the frameworks of the desired topologies and controlling the pore sizes, dimensions, functionalities, and applications. It is expected that the establishment of these few nCOFs will initiate the rebounding interest in the exploration of functional porous nCOF materials for their potential applications.

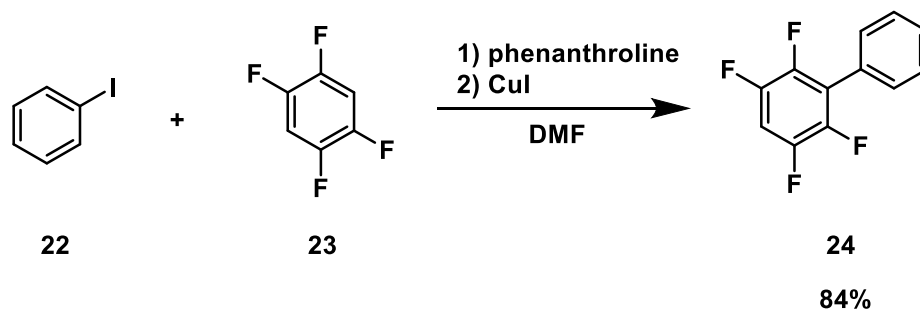
2.5 Experimental Section

2.5.1 General Methods

All reagents were purchased from commercial suppliers and used without further purification. Solvents were used as received, except tetrahydrofuran (THF), which was dried over activated alumina in an mBraun solvent Purification System. Triethylamine (Et_3N) was distilled over KOH pellets. All solvents were degassed by a 20 min nitrogen purge prior to use. ^1H and ^{19}F NMR spectra were recorded on JEOL ECA-500 or ECX-400 spectrometers using the peaks of TMS or residual solvent as standards. Trifluorotoluene (PhCF_3 , $\delta = -63.72$ ppm) was used as the internal standard in ^{19}F NMR

spectra. All ^{13}C NMR spectra were recorded with simultaneous decoupling of ^1H nuclei. ^1H NMR chemical shifts are reported in ppm units relative to the residual signal of the solvent (CDCl_3 : 7.26 ppm), and multiplicity is expressed as follows: s = singlet, d = doublet, m = multiplet. All NMR spectra were recorded at 25 $^\circ\text{C}$. Mass spectral measurements were performed by the Mass Spectrometry Facility of the Department of Chemistry at the University of Houston. Infrared spectra were recorded on a Perkin-Elmer Spectrum 100 FT-IR spectrophotometer using Pike MIRacle Micrometer pressure clamp. Microanalyses were conducted by Intertek USA, Inc. Melting points were measured in open capillary tubes using Mel-Temp Thermo Scientific apparatus and are uncorrected. Column chromatography was carried out on silica gel 60, 32–63 mesh. Analytical TLC was performed on JT Baker plastic-backed silica gel plates.

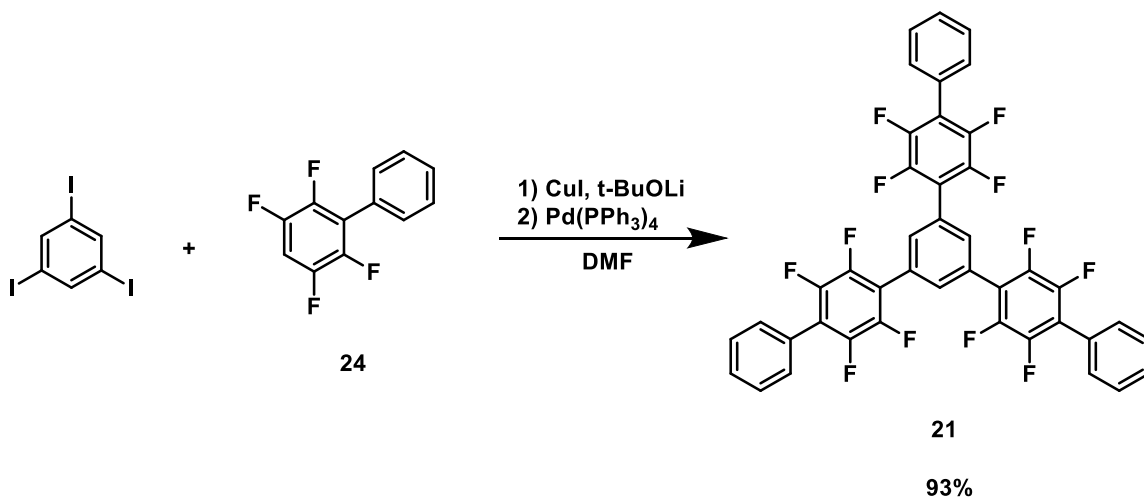
2.5.2 Synthesis of 2,3,5,6-Tetrafluoro-1,1'-Biphenyl (**24**)



Outside the glovebox, a 1-dram vial equipped with a magnetic stir bar was charged with phenanthroline (720 mg, 4 mmol), CuI (768 mg, 4 mmol), iodobenzene **22** (8.16 g, 40 mmol), 1,2,4,5-tetrafluorobenzene **23** (18 g, 120 mmol), and DMF (10.0 mL). The vial was flushed with nitrogen, capped and placed inside a glovebox. To this mixture

was added *t*-BuOLi (6.28 g, 56 mmol). The sealed vial was then taken out of the glovebox and stirred at 125 °C for 24 hours. The reaction mixture was cooled to room temperature and subjected to column chromatography on silica gel. After column chromatography (hexanes) 7.8 g (84%) of the white solid product was obtained. Spectral data were consistent with literature reports.³⁹

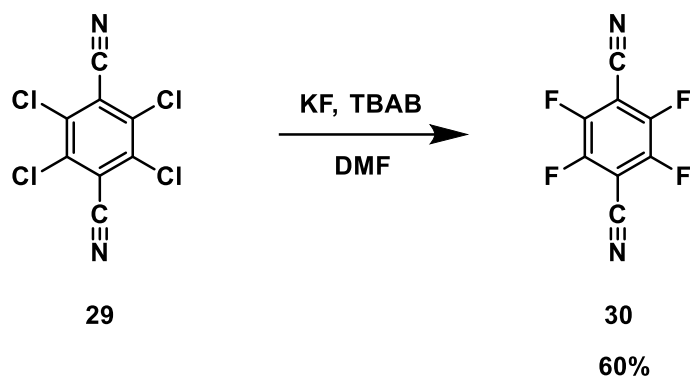
2.5.3 Synthesis of 1,3,5-Tris<(2,3,5,6-Tetrafluoro-4-Phenyl)-Phenyl>Benzene (21)



A 100 mL screw cap pressure vessel was equipped with a magnetic stir bar and charged with CuI (6.38 g, 33.5 mmol) and *t*-BuOLi (2.68 g, 33.5 mmol). Dry DMF (40 mL) was added, and the vessel was sealed, taken out of the glovebox, sonicated for 5 min and vigorously stirred at 25 °C for 1 h. The pressure vessel was then placed back inside the glovebox, and 2,3,5,6-tetrafluoro-1,1'-biphenyl **24** (7.7 g, 34.0 mmol) was added in one portion. After that, the reaction vessel was sealed again, taken out of the glovebox, sonicated for 5 min and vigorously stirred at 25 °C for 1 h. The pressure vessel was placed back inside the glovebox. Catalyst Pd(PPh₃)₄ (347 mg, 0.30 mmol) was added,

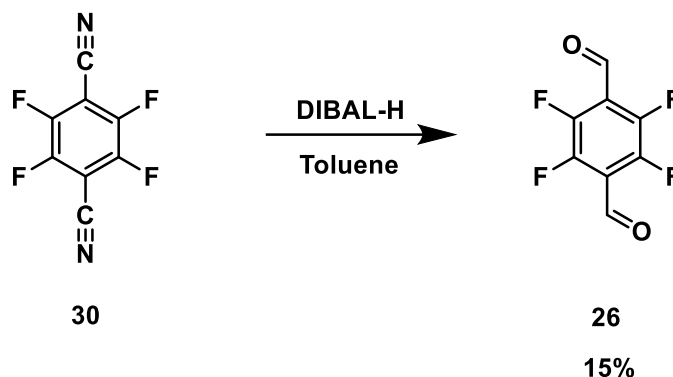
followed by 1,3,5-triiodobenzene (4.56 g, 10 mmol). The reaction vessel was sealed, taken out of the glovebox and placed inside an oil bath preheated to 100 °C, where it was stirred vigorously for 12 h. Reaction mixture was cooled to 25 °C, diluted with DCM (150 mL) and 3% aqueous citric acid (100 mL) was added. After filtration through a plug of celite, the filter cake was washed with additional DCM (3×25 mL). Combined organic layers were separated and washed with deionized water (5×100 mL), followed by brine (100 mL). The organic layer was dried over anhydrous MgSO₄, filtered and dry-absorbed on silica gel. After purification by column chromatography on silica gel using DCM/hexanes as eluent and evaporation of the fractions containing the product, compound **21** was obtained as white solid (6.9 g, 93%). m.p. of compound **21** is over 260 °C. IR (neat): 1682 (w), 1602 (w), 1489 (m), 1475 (w), 1420 (m), 1309 (w), 1136 (w), 71 (s), 733 (w), 694 (s) cm⁻¹. ¹H NMR (CDCl₃, 500 MHz): δ 7.82 (s, 1H), 7.55 (m, 5H) ppm. ¹³C NMR (CDCl₃, 125 MHz): δ 145.27, 143.31, 132.66, 130.26, 129.42, 128.78, 128.71, 127.35, 120.68, 118.05 ppm. ¹⁹F NMR (CDCl₃, 470 MHz): δ -143.36 to -143.43 (q, 6F), -143.86 to -143.94 (q, 6F) ppm.

2.5.4 Synthesis of 1,4-Dicyano-2,3,5,6-Tetrafluorobenzene (**30**)



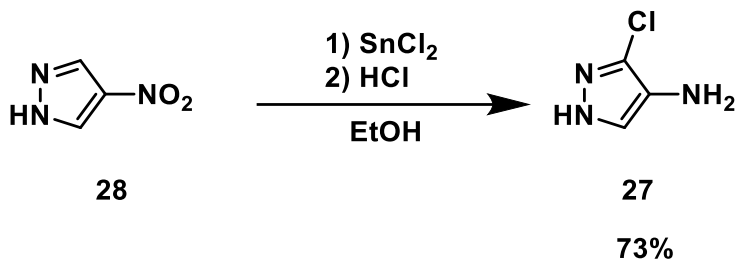
Compound 1,4-dicyano-2,3,5,6-tetrachlorobenzene **29** (20 g, 0.075 mol), KF (21.7 g, 0.19 mol), and tetrabutylammonium bromide (TBAB) (0.99 g, 2 mol%) were added to a flask containing dry DMF (125 mL), and the mixture was stirred overnight at 120 °C under N₂. Then the reaction mixture was poured into a beaker with 1 L of ice-water, and the resulting precipitate was filtered and washed with water. The crude product was recrystallized from acetone to give the yellowish white pure product **30** (9.8 g, 68%). Spectral data were consistent with literature reports.⁴⁰

2.5.5 Synthesis of 2,3,5,6-Tetrafluorobenzene-1,4-Dicarbaldehyde (**26**)



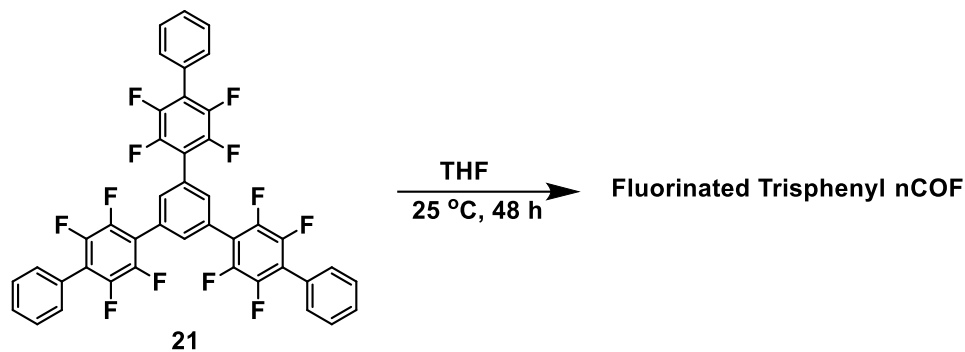
To a solution of 1,4-dicyano-2,3,5,6-tetrafluorobenzene **30** (10.0 g, 0.05 mol) and toluene (150 mL) at 0 °C was added 125 mL (0.125 mol) of 1 M DIBAL-H (diisopropylaluminum hydride) hexane solution dropwise under N₂. The mixture was stirred at 0 °C for 1 h and then was slowly warmed to room temperature and stirred overnight. The reaction was quenched by addition of 150 mL of 2 N HCl until pH <2, and then the mixture was stirred for another 30 min. The resulting precipitate was filtered and washed with DCM, and the aqueous layer was extracted with DCM (6×50 mL). The organic layer was washed with saturated sodium bicarbonate and brine, dried over MgSO₄, and evaporated, and the crude product was further purified recrystallized from DCM to give product **26**, 1.55 g (yield 15%). Spectral data were consistent with literature reports.⁴⁰

2.5.6 Synthesis of 3-Chloro-1H-Pyrazol-4-Amine (27)



A 1 L Schlenk flask was flushed with nitrogen and charged with nitroaniline **28** (6.00 g, 30.3 mmol), concentrated HCl (311 mL), and EtOH (155 mL). The reaction flask was attached to the condenser and heated at 50 °C with stirring for 10 min. After 10 min, a solution of anhydrous SnCl_2 (52.0 g, 274 mmol) in EtOH (80 mL) was added to the reaction mixture. The beaker containing the SnCl_2 solution was washed with an additional portion of EtOH (40 mL), and the washings were added to the reaction flask. The reaction was heated to 86 °C for 24 hours to ensure that the reaction went to completion. The reaction resulted in a white precipitate forming in the flask. After cooling, the solution was filtered and the residue was washed with EtOH to give the product **27** as a light pink solid (8.1 g). The crude product was used without further purification. The m.p. of this compound **27** is 54 °C. IR (neat): 3335 (w), 3271 (w), 3116 (m), 2966 (w), 2872 (m), 1574 (m), 1417 (s), 1352 (m), 1313 (w), 1172 (m), 1103 (m), 900 (s), 801 (s) cm^{-1} . ^1H NMR ($\text{DMSO}-d_6$, 500 MHz): δ 12.18 (s, 1H), 7.09 (s, 1H), 3.80 (br, 2H) ppm. ^{13}C NMR ($\text{DMSO}-d_6$, 125 MHz): δ 128.78, 126.56, 117.24 ppm.

2.5.7 Synthesis and Characterization of Fluorinated Trisphenyl nCOF



Ligand **21** (5 mg, 0.007 mmol) was dissolved in 1.5 mL of solvent THF in a 4 mL vial. The vial was sealed by a septum with a 18 G needle connecting to the atmosphere. The solvent slowly evaporated at 25 °C for 48 h. After most of the solvent was evaporated, crystalline materials were formed and then washed several times with fresh MeOH. Finally, the white transparent hexagonal-shaped crystals were produced, which were characterized with single crystal X-ray crystallography.

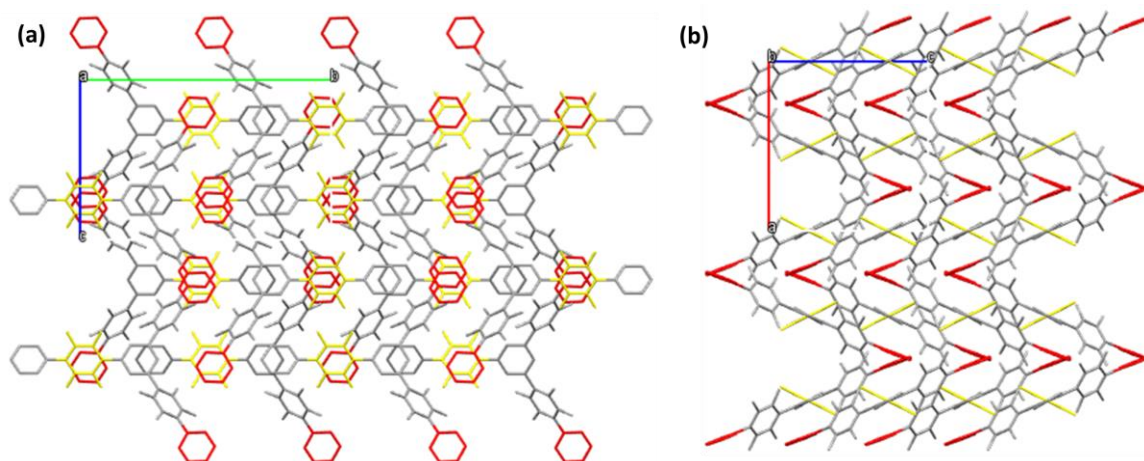


Figure 2.6 (a) 3D network of fluorinated trisphenyl nCOF along *a* axis, red and yellow stand for π - π related terminal phenyl rings and tetrafluorobenzene rings; (b) 3D network of fluorinated trisphenyl nCOF along *b* axis.

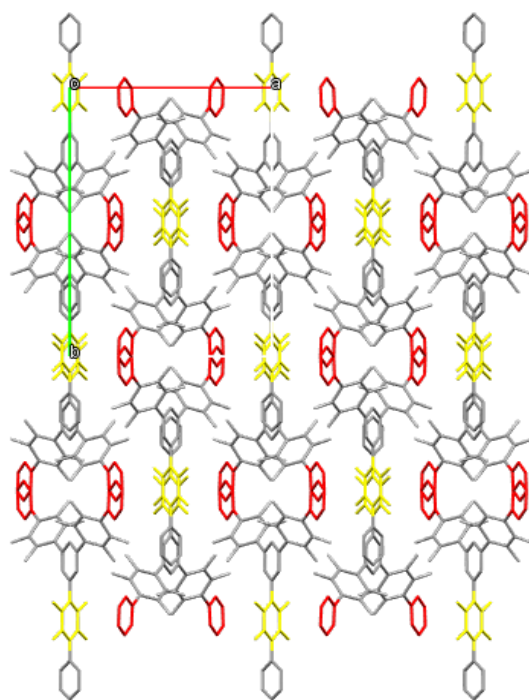
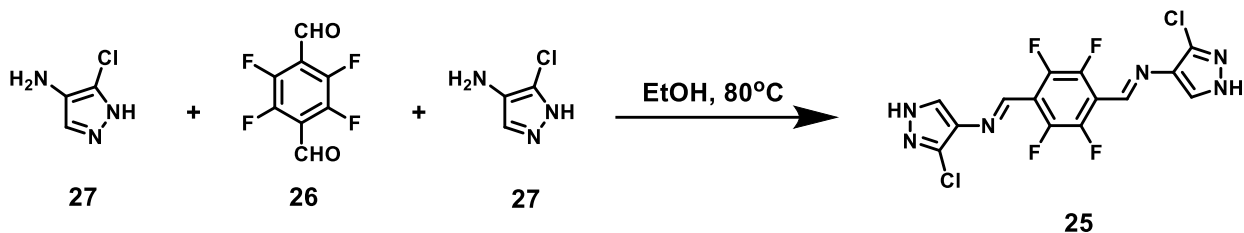


Figure 2.7 3D network of fluorinated trisphenyl nCOF along crystallographic *c* axis. Red and yellow stand for π - π related terminal phenyl rings and tetrafluorobenzene rings.

2.5.8 Synthesis and Characterization of Linear Imine-Based nCOF



Compound **26** (3.09 mg, 0.015 mmol) with two equivalents of compound **27** (3.54 mg, 0.03 mmol), were mixed in 1.5 mL solvent of EtOH in a 4 mL vial. The vial was sealed with Teflon tape, capped firmly, and then heated in the oven at 80 °C for 12 h. The solvent was removed afterwards, and resulting yellow crystalline materials were washed several times with fresh MeOH. The crystals were characterized with single crystal X-ray crystallography. The m.p. of compound **25** is over 260 °C. IR (neat): 3180 (w, $\tilde{\nu}_{\text{N-H}}$), 3095 (w, $\tilde{\nu}_{\text{C-H}}$), 1602 (w), 1507 (w), 1480 (s), 1362 (m), 1306 (m), 1172 (m), 1110 (m), 1027 (s), 647 (m) cm^{-1} .

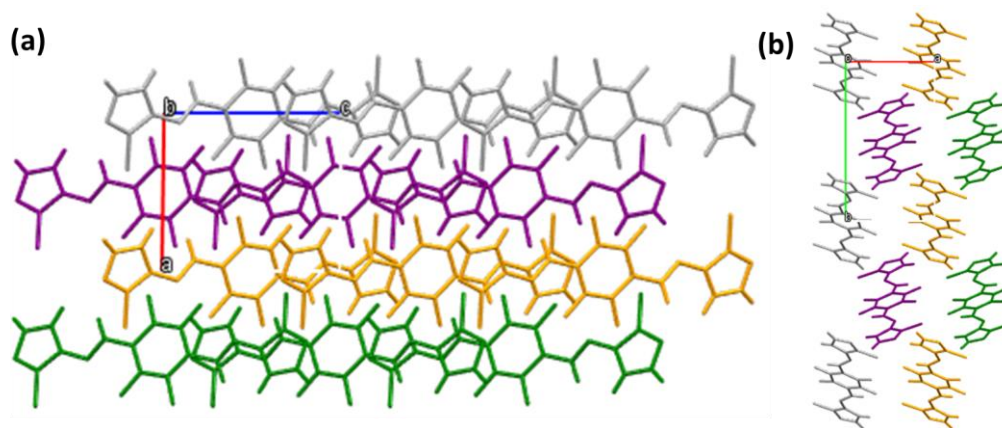


Figure 2.8 (a) 3D network of linear imine-based nCOF along *b* axis; (b) 3D network of linear imine-based nCOF along *c* axis. Each color represents an independent 1D chain.

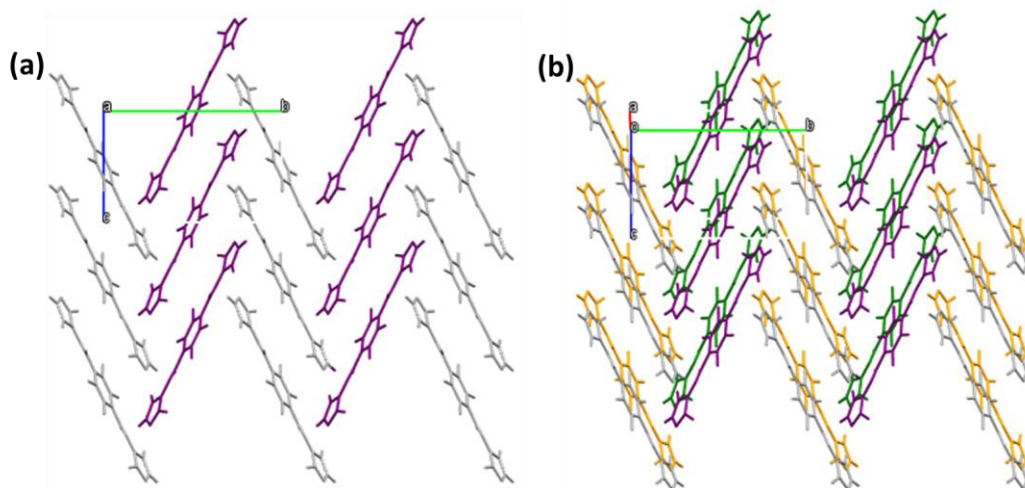


Figure 2.9 (a) 3D network of linear imine-based nCOF along *a* axis. Colored ligands form 1D chain through π - π stacking; (b) Each 1D chain is connected through hydrogen bonding along *a* axis.

Chapter Three

Self-Sorting of Complex Libraries during Kinetically Controlled Acylations

3.1 Introduction to Self-Sorting

Sorting, in general, is any process of arranging items systematically, and has two common, yet distinct meanings: ordering and categorizing, i.e., to arrange items in a sequence ordered by some criterion as well as to group items with similar properties.

Self-sorting is then a process of spontaneous and high-fidelity recognition of related compounds within a complex mixture, based on their behaviors and socialization.⁴¹ Most examples of self-sorting are reversible interactions, such as metal-ligand coordination,⁴² hydrogen bonding,⁴³ or dynamic covalent chemical reactions.⁴⁴ To date, self-sorting has been observed in still a small number of designed molecular systems while it is commonplace in biological systems. The phenomenon of self-sorting is common in nature, as many natural processes must carry out self-sorting to build up selective functions while being hindered by the surrounding agents which are simultaneously competing. They require very efficient molecular recognition and discrimination to ensure correct stoichiometry and proper structure of the final product, as otherwise the desired function will not emerge.⁴⁵

Self-sorting processes can occur under thermodynamic or kinetic control. The former is a reversible process: chemical exchange is ongoing and the self-sorted state is simultaneously the lowest-energy state of the system. The latter is an irreversible process,

in which the self-sorted state is the one that emerges the fastest, without regard to its relative stability compared to the other states of the system (Figure 3.1). Thermodynamically controlled self-sorting has been extensively studied during the past decade, such as Diels-Alder/retro-Diels-Alder reaction, trans-esterification as well as imine exchange.^{46,47} They usually require conditions of high temperature and long reaction time to guarantee the reversibility during the reaction and eventually produce a collection of molecules which are the best pairs to each other.

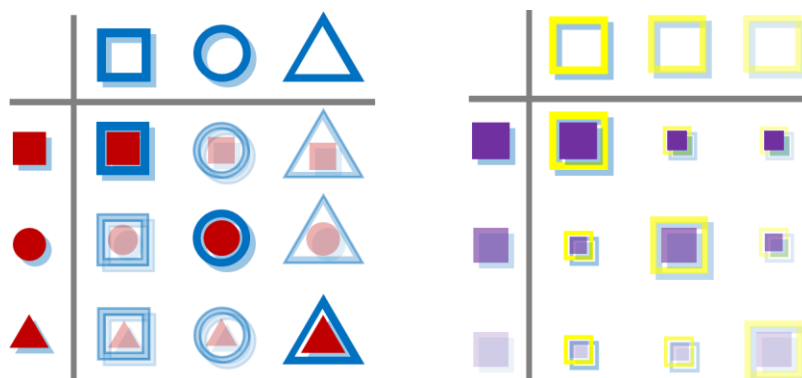


Figure 3.1 Schematic representations of thermodynamically controlled self-sorting (left); and kinetically controlled self-sorting (right). The opaque combinations represent major products while the transparent combinations represent minor ones.

Among the kinetically controlled self-sorting phenomena reported by our group, we have shown that an irreversible stimulus for the self-sorting, both chemically and physically can be used to achieve simplification of complex into a handful of discrete high-purity products.⁴⁸ One of the most recent example is a mixture of 16 esters being dynamically transesterified in the presence of catalyst $\text{Ti}(\text{OBu})_4$, and then, during the course of a vacuum distillation of this mixture as a physical stimulus, the original 16

components (initially present in an equimolar ratio) were self-sorted into 4 products based on their different boiling points (Figure 3.2).⁴⁹ Distillation of this mixture will isolate the most volatile ethyl acetate **31** in 87% yield, formed from the most volatile acid and the most volatile alcohol (shown in red). As two most volatile parts being removed, the equilibrium keeps shifting until four equivalents of both parts have been consumed completely. The reaction system will then continue producing the second most volatile ester—butyl butyrate **32**—in 88% yield, followed by octyl octanoate **33** in 70% and cetyl palmitate **34** in 85% yields. In essence, this protocol produces four well-defined products in high purity and good yields—all while starting from a complex “messy” mixture of sixteen starting materials.

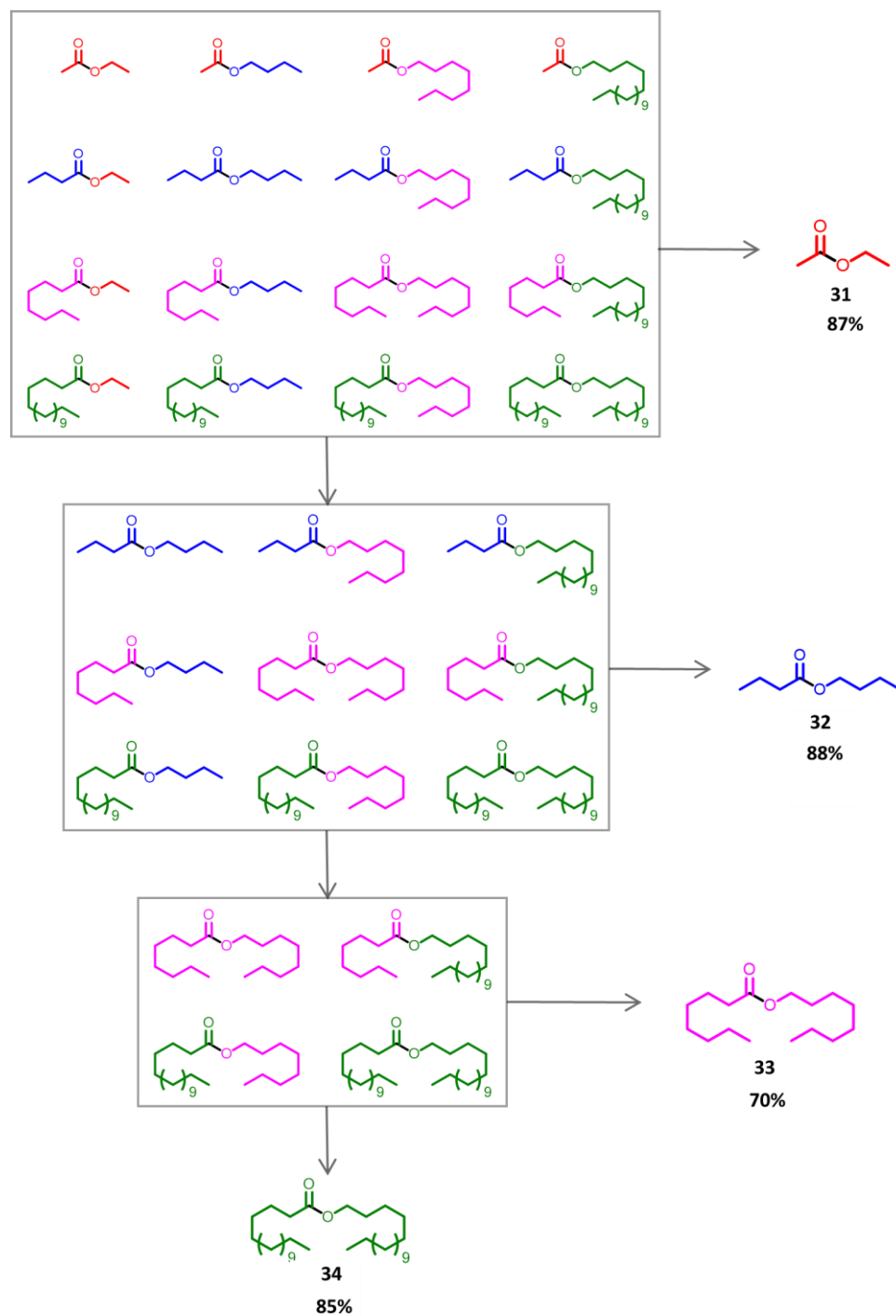


Figure 3.2 Self-sorting of a dynamic [4x4] ester library during reactive distillation. The molecular pieces shown in red are sorted out of the reaction mixture first; followed pieces in blue, pink and green.

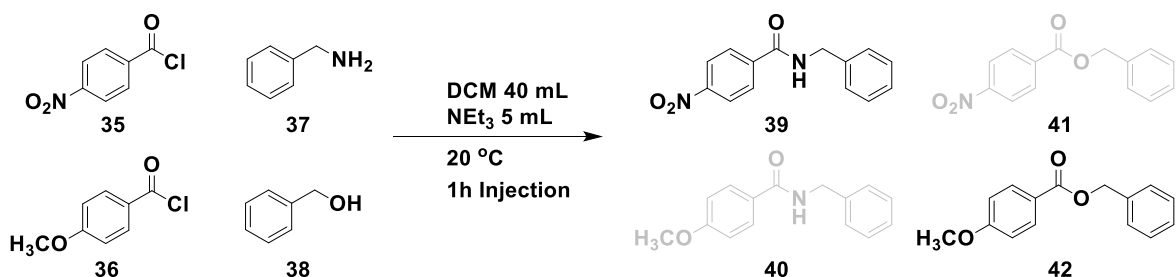
Encouraged by the success of this work, we directed our efforts at identifying self-sorting behaviors in mixtures where there is no underlying equilibration among the precursors. In other words, we wondered whether more challenging self-sorting processes—dominated entirely by kinetically controlled and highly exergonic chemical reactions—could be identified and productively utilized. Among these were kinetically-controlled acylations to form amides, esters, and thioesters; these reactions normally proceed very rapidly and rather unselectively, but control may be achieved by employing milder conditions or using substrates with sufficient reactivity differences. The following section will describe our efforts in kinetically controlled acylation self-sorting processes.

3.2 Results and Discussion

3.2.1 Selectivity Tests in [2×2] Self-Sorting Systems

Our initial studies of this kinetically controlled self-sorting acylation focused on four substrates: *p*-nitrobenzoyl chloride **35**, *p*-methoxybenzoyl chloride **36**, benzylamine **37**, and benzyl alcohol **38** (Scheme 3.1). Among the possible products from this reaction system were amides **39** and **40**, and esters **41** and **42**. With equimolar ratio of all four starting materials, selective self-sorting process should have resulted in an exclusive formation of **39** and **42**. This is because the electron-poor acyl chloride **35** is more reactive than the electron-rich **36**, while nucleophile **37** with a higher pK_a value is stronger than **38**. Thus **35** and **37** will pair with each other first producing **39**, and left **36** and **38** to have no option but form **42**. The result was analyzed by ^1H NMR with internal standard, and we found that all *p*-nitrobenzoyl chloride **35** and benzylamine **37** were

consumed completely but a large percentage of *p*-methoxybenzoyl chloride **36** and benzyl alcohol **38** stayed unreacted. Therefore, a mixture of four different products and two leftover starting materials were obtained. To make the reaction proceed to completion, we tried heating the resulting solution after injection. NMR spectroscopy showed the same result again. We then added an excess amount of *p*-methoxybenzoyl chloride **36** to the resulting solution after *p*-nitrobenzoyl chloride **35** and benzylamine **37** were fully consumed. This time we found all four starting materials go to the products with a promising selective formation of 76% **39**, 15% **41**, 11% **40**, and 77% **42**, respectively. We were able to see the “sorting” as expected, even though we had to add an extra equivalent of the *p*-methoxybenzoyl chloride **36**.



Scheme 3.1 Kinetically controlled acylation self-sorting of a [2×2] system.

Next, we switched from benzyl alcohol **38** to pyrrolidine **43** as the nucleophilic substrate (Figure 3.3). We used exactly same conditions as in the previous example to run the new [2×2] reaction. In this adapted system, all four reactants had been totally consumed even when their initial amounts were equimolar. However, the selectivity is not high enough, as the respective yields of products were 75% of **39**, 24% of **41**, 23% of **44**, and 73% of **45**.

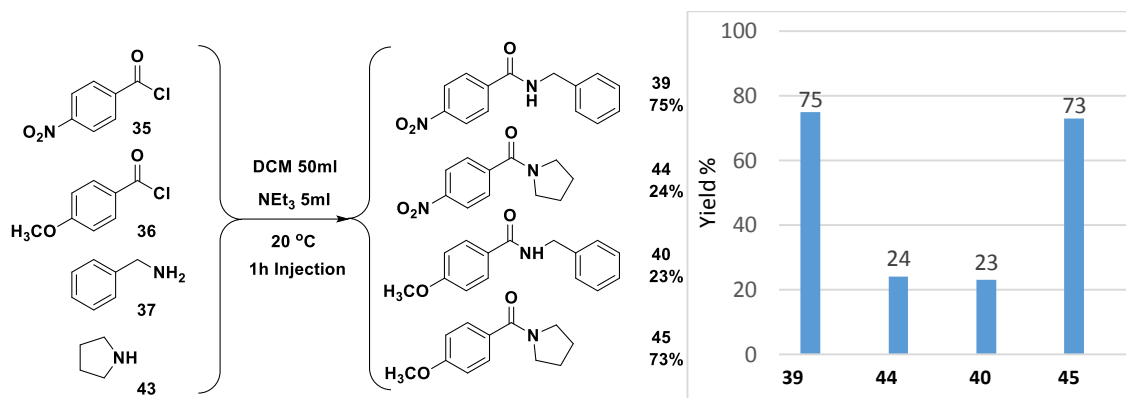


Figure 3.3 Acylation self-sorting in a new [2×2] system and its selective results.

3.2.2 Optimization of Acylation Self-Sorting Conditions

After we achieved this promising result without the addition of any extra substrates, we decided to vary our experimental conditions to optimize the selectivity. Temperature as first impact factor came to our mind. We used the previous successful combinatorial library — *p*-nitrobenzoyl chloride **35**, *p*-methoxybenzoyl chloride **36**, benzylamine **37**, and pyrrolidine **43**, and only varied the temperature on $-78\text{ }^{\circ}\text{C}$, $-20\text{ }^{\circ}\text{C}$, $0\text{ }^{\circ}\text{C}$, $20\text{ }^{\circ}\text{C}$, $40\text{ }^{\circ}\text{C}$, to, while other experimental conditions the same from the original [2×2] system (Figure 3.4 Temperature). For the first series of optimization, to our surprise we figured out that best selectivity came out of the $0\text{ }^{\circ}\text{C}$ system, however, the difference among the systems at various temperatures is not very significant. This may be because, mechanistically, acylation reaction will be affected by not only the temperature, but also the stability, polarizability, and electronic property of the reacting substrate. Therefore, different acylation reaction rate are not equally decreasing and overall the best selectivity came out at $0\text{ }^{\circ}\text{C}$ within that temperature range.

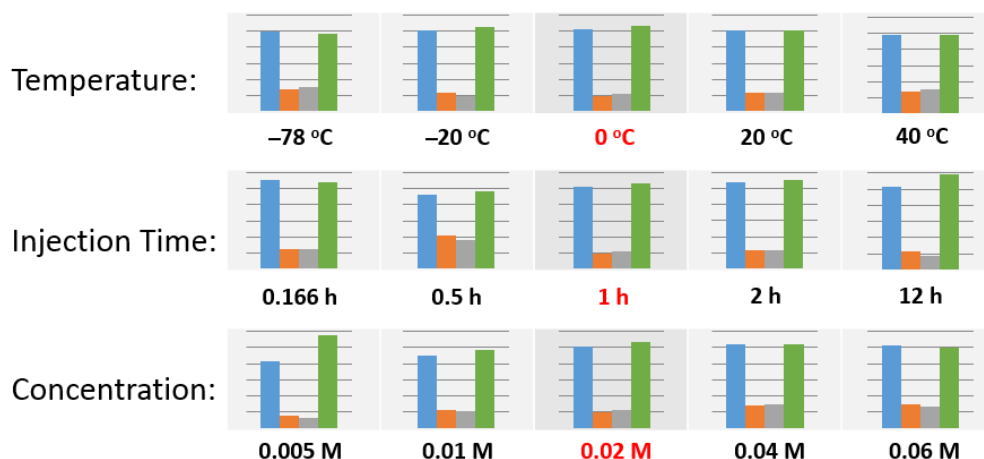


Figure 3.4 Temperature (first row), injection speed (second row), concentration (third row) variation experiments in a $[2 \times 2]$ self-sorting system. Best conditions are highlighted in red.

For the second series of optimization we tested different injection rates. By fixing every factors and just varying injection time from as short as 10 min to as long as 12 hours, we did not find any trend this time (Figure 3.4 Injection time), thus we decided to keep using 1 hour as the injection time for remaining experiments. In the third series of variations, starting materials' amount had been changed from using 1 mmol to 2 mmol, 3 mmol, 0.5 mmol and 0.25 mmol. Variations in these concentration experiments did not result in significant changes as well in this selectivity (Figure 3.4, concentration). We conclude from our optimization experiments that these acylation reactions are highly exothermic processes and will not be significantly affected by the external conditions, so that we continued using our initial conditions: 0 °C, 1 hour injection, and 0.02 M as reagent concentration for acylation self-sorting.

3.2.3 Substrate Reactivity Arrangement

Encouraged by the relative success of [2×2] self-sorting systems, we performed a series of experiments aimed at arranging the nucleophiles and acyl chlorides in order of their reactivities. Using a standardized [2×2] acylation reaction, we fixed two acyl chlorides **35** and **36**, and used benzylamine **37** as the nucleophile reference, while varying the other nucleophile reactant. In the very first [2×2] system, I was able to get an approximate 1 to 3 (23% to 75%) selectivity in both sides (red and blue), however, since we would use a 1D reactivity list, this 1/3 ratio value had to be recalculated under logarithm function (Figure 3.5). Therefore, $\log_{10}(23\%/75\%) = -0.513$, and pyrrolidine **43** could then be assigned in the reactivity list using benzylamine **37** as the reference.

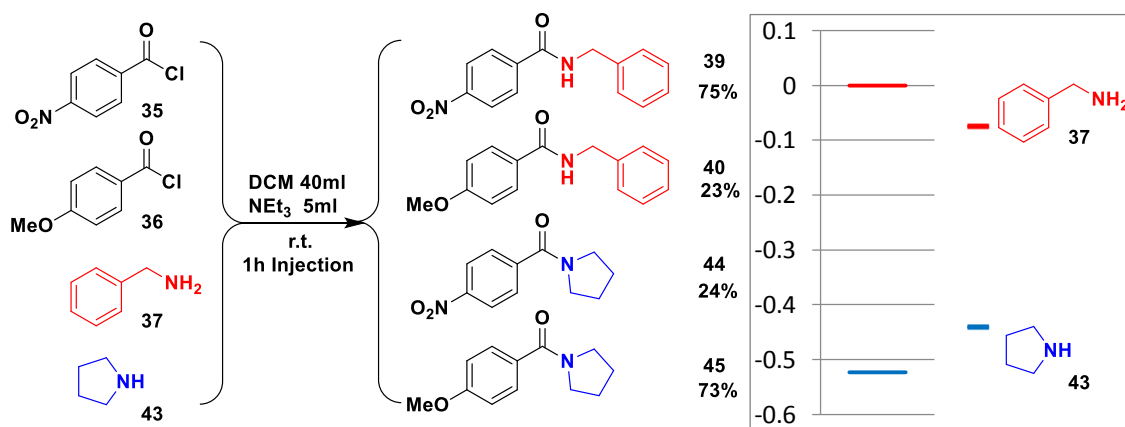


Figure 3.5. Nucleophile reactivity test conditions and reactivity list assignment.

3.2.3.1 Establishment of Nucleophiles' Reactivity List

We continued using the same system consisting of acyl chlorides **35** and **36**, and benzylamine **37** as the fixed components, while varying the second nucleophile from

alcohols to amines to thiols. Eventually, all nucleophiles would be compared to benzylamine **37** and then be assigned a position in the reactivity list (Figure 3.6).

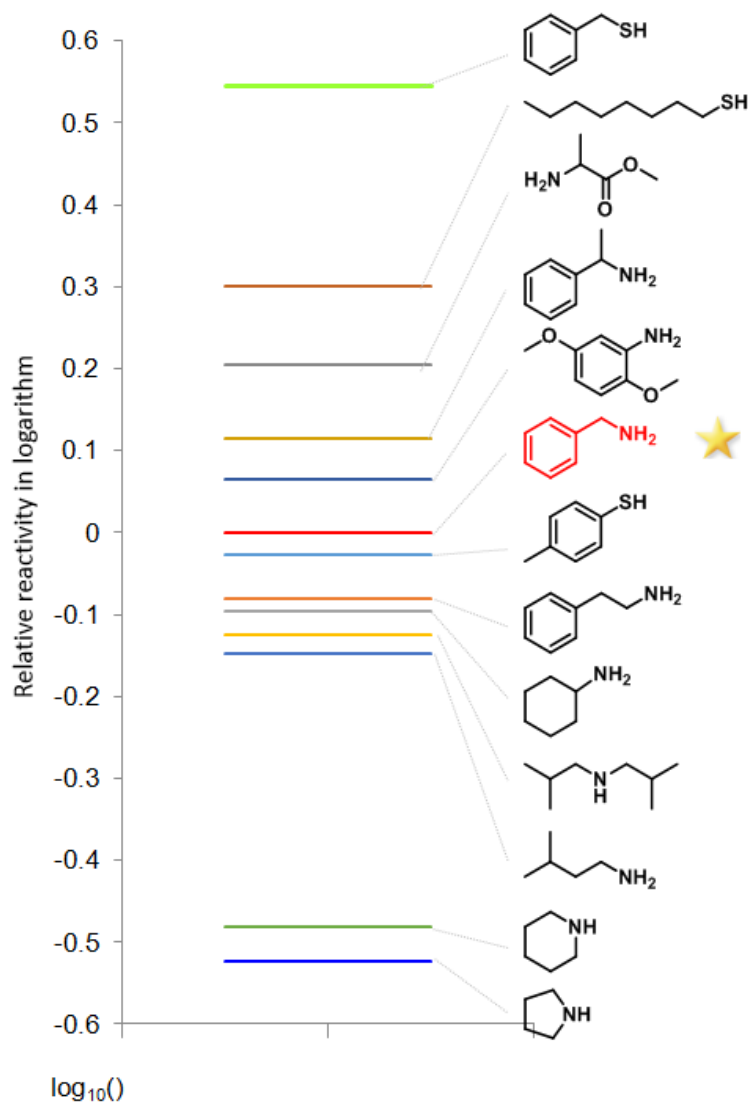


Figure 3.6 Nucleophiles' reactivity list of 13 compounds. Benzylamine **37** marked by a yellow star was treated as reference in the test.

3.2.3.2 Establishment of Acyl Chlorides' Reactivity List

We also used *p*-methoxybenzoyl chloride **36** as the acyl chloride reference, plus benzylamine **37**, and pyrrolidine **43** as the fixed components to arrange all the acyl chlorides into another list (Figure 3.7).

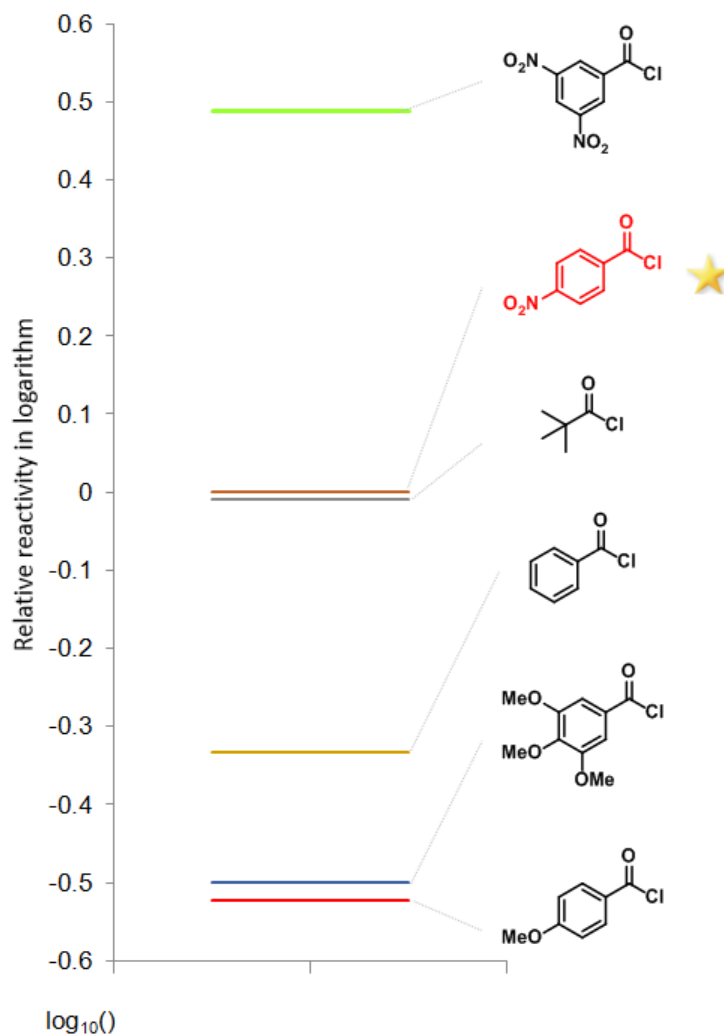


Figure 3.7 Acyl chlorides' reactivity list of 6 compounds. *p*-methoxybenzoyl chloride **36** marked by a yellow star was treated as reference in this test.

3.2.4 Selectivity Tests in [3×3] Self-Sorting Systems

After we compiled these two reactivity lists, we used the three nucleophiles with biggest reactivity differences based on our findings (benzyl mercaptan **46**, benzylamine **37**, and pyrrolidine **43**) and three acyl chlorides (3,5-dinitrobenzoyl chloride **47**, pivaloyl chloride **48**, p-methoxybenzoyl chloride **36**) to run a [3×3] reaction. The results showed that the most reactive acyl halide **47** found the strongest nucleophile **46** first and formed the thioester product **49** with 82% yield, and the second most reactive pair **48** and **37** followed to form the amide product **50** with 70% yield, and finally the least reactive pair **36** and **43** formed another amide product **45** with 80% yield (Figure 3.8). We also succeeded in obtaining reasonable selectivity in other [3×3] systems consisting of components with sufficient reactivity differences.

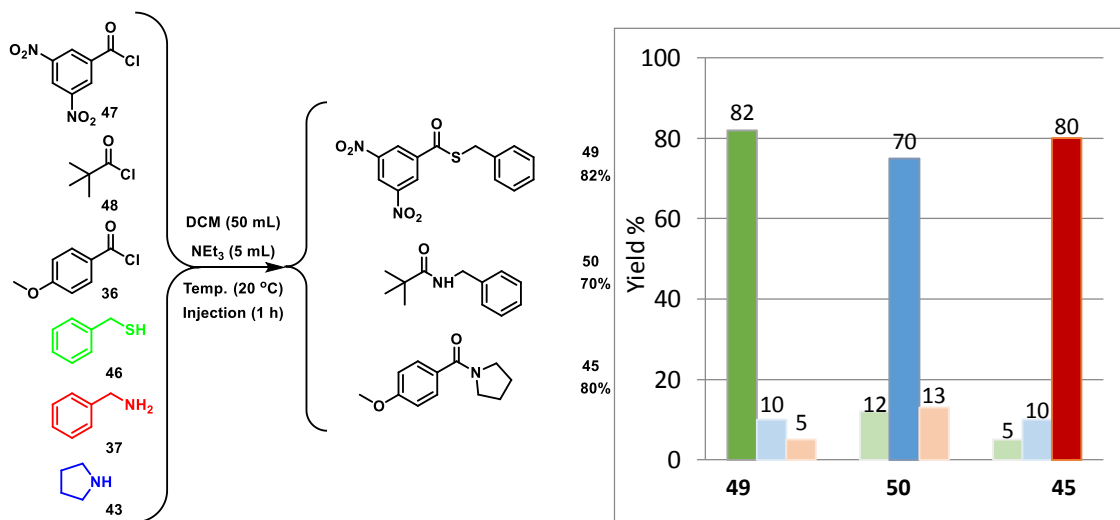


Figure 3.8 Acylation self-sorting in a [3×3] system.

3.3 Conclusion and Outlook

The more-challenging molecular recognitions: absolute kinetically controlled self-sortings have been established in several [2×2] and [3×3] mixtures. These selective series of acylations can proceed with less than 20% interference from the undesired “crossover” products. Among these were amide, ester, and thioester formations; these reactions normally proceed very rapidly and rather unselectively, but control was achieved by optimization of experimental conditions and utilizing substrates with sufficient reactivity differences. The library of possible substrates for acylation reactions have been also built. Every nucleophile and acyl chloride is assigned a position in the list based on their reactivity. This accomplishment was enabled by the thorough understanding of relative reactivities of various nucleophiles and acyl chlorides.

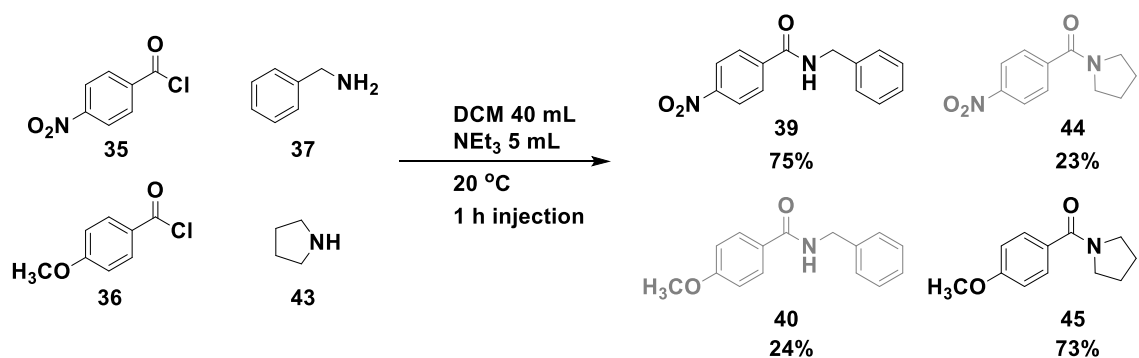
3.4 Experimental Procedures

3.4.1 General Synthetic and Characterization Methods

All reactions were performed under nitrogen atmosphere in oven-dried glassware. All reagents were purchased from commercial suppliers and used without further purification. Solvents were used as received, except dichloromethane (DCM), which was dried over anhydrous calcium chloride (CaCl₂) in an mBraun solvent Purification System. Triethylamine (Et₃N) and diisopropylamine (*i*-Pr₂NH) were distilled over KOH pellets. ¹H NMR spectra were obtained on JEOL ECX-400 and ECA-500 spectrometers, with working frequencies of 400 and 500 MHz, respectively. All ¹³C NMR spectra were

recorded with simultaneous decoupling of ^1H nuclei. ^1H NMR chemical shifts are reported in ppm units relative to the residual signal of the solvent (CDCl_3 : 7.26 ppm), and multiplicity is expressed as follows: s = singlet, d = doublet, m = multiplet. All NMR spectra were recorded at 25 $^\circ\text{C}$. NMR yields were calculated by adding approx. 1.0 equivalent of 1,3,5-trimethoxybenzene (Alfa Aesar, 99%) as the internal standard to the crude reaction mixture. Infrared spectra were recorded on a Perkin-Elmer Spectrum 100 FT-IR spectrophotometer using Pike MIRacle Micrometer pressure clamp. Melting points were measured in open capillary tubes using Mel-Temp Thermo Scientific apparatus and are uncorrected. Column chromatography was carried out on silica gel 60, 32–63 mesh. Analytical TLC was performed on JT Baker plastic-backed silica gel plates.

3.4.2 Selected Self-Sorting Experimental Procedure of [2 \times 2] Acylation Mixture



Equimolar amounts of *p*-nitrobenzoyl chloride **35** (188 mg, 1.00 mmol) and *p*-methoxybenzoyl chloride **36** (170 mg, 1.00 mmol) were mixed in anhydrous DCM (5 mL) and then transferred into a 5 mL syringe. Separately, benzylamine **37** (107 mg, 1.00 mmol) and pyrrolidine **43** (71 mg, 1.00 mmol) were mixed in anhydrous DCM (5 mL) and

transferred into another 5 mL syringe. Two syringes were placed into a syringe pump with injection rate set to 5 mL/h. A Schlenk flask (100 mL) was dried overnight in the oven and then backfilled with N₂ before anhydrous DCM (40 mL) and NEt₃ (5 mL) were added to it. The two syringes were connected to the Schlenk flask through two needles (20 G) and Teflon tubing. The four starting materials were slowly injected at room temperature to the solution in the flask over 1 h. After the injection finished, 2 mL out of 55 mL solution were used for characterization by NMR spectroscopy, with trimethoxybenzene (12.1 mg, 0.074 mmol) as the internal standard. ¹H NMR analysis showed the identity of products as a mixture of benzyl *p*-nitrobenzamide **39** (75% yield), (*p*-nitrophenyl)(pyrrolidin-1-yl)methanone **44** (23% yield), benzyl *p*-methoxybenzamide **40** (24% yield), and (*p*-methoxyphenyl)(pyrrolidin-1-yl)methanone **45** (73% yield).

3.4.3 Other Selective Acylation Self-Sorting in [2×2] Systems

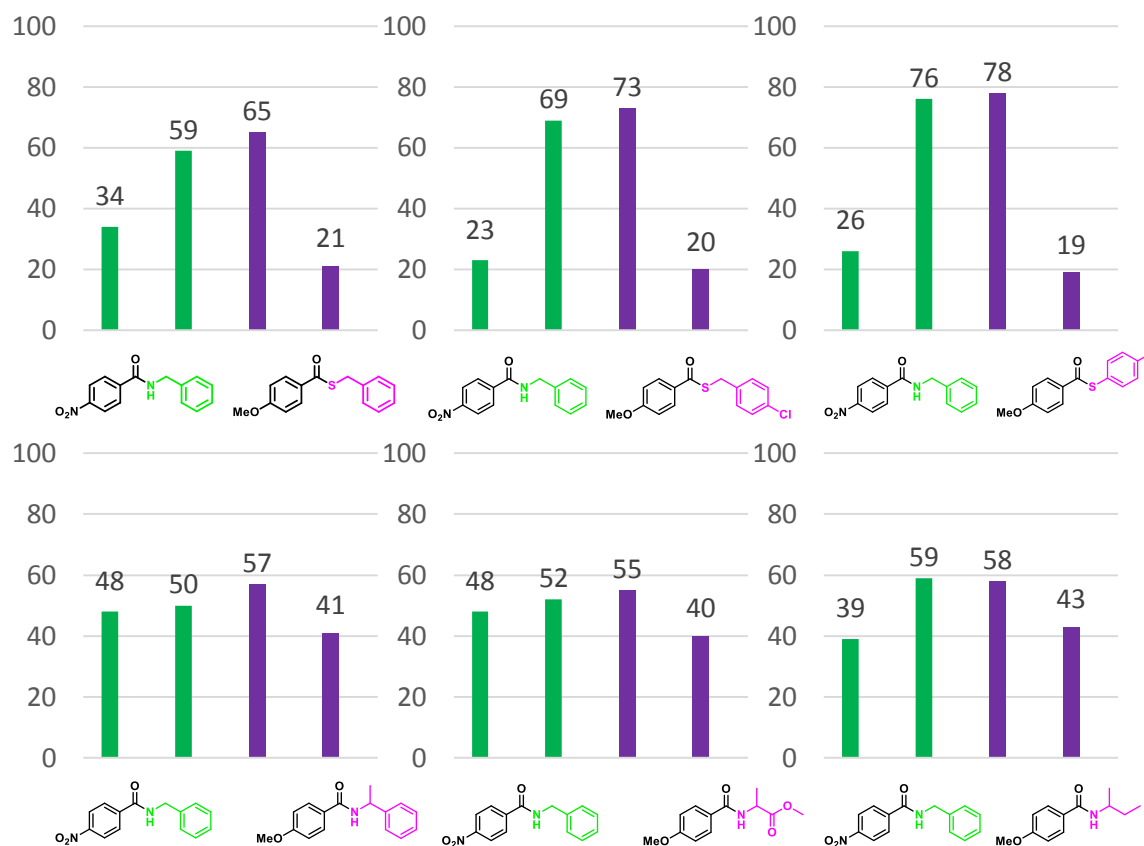


Figure 3.9 Self-sorting in [2×2] systems with fixed two acyl chlorides **35**, **36**, and benzylamine **37** while varying the other nucleophile (purple substrate). Only major compounds are shown.

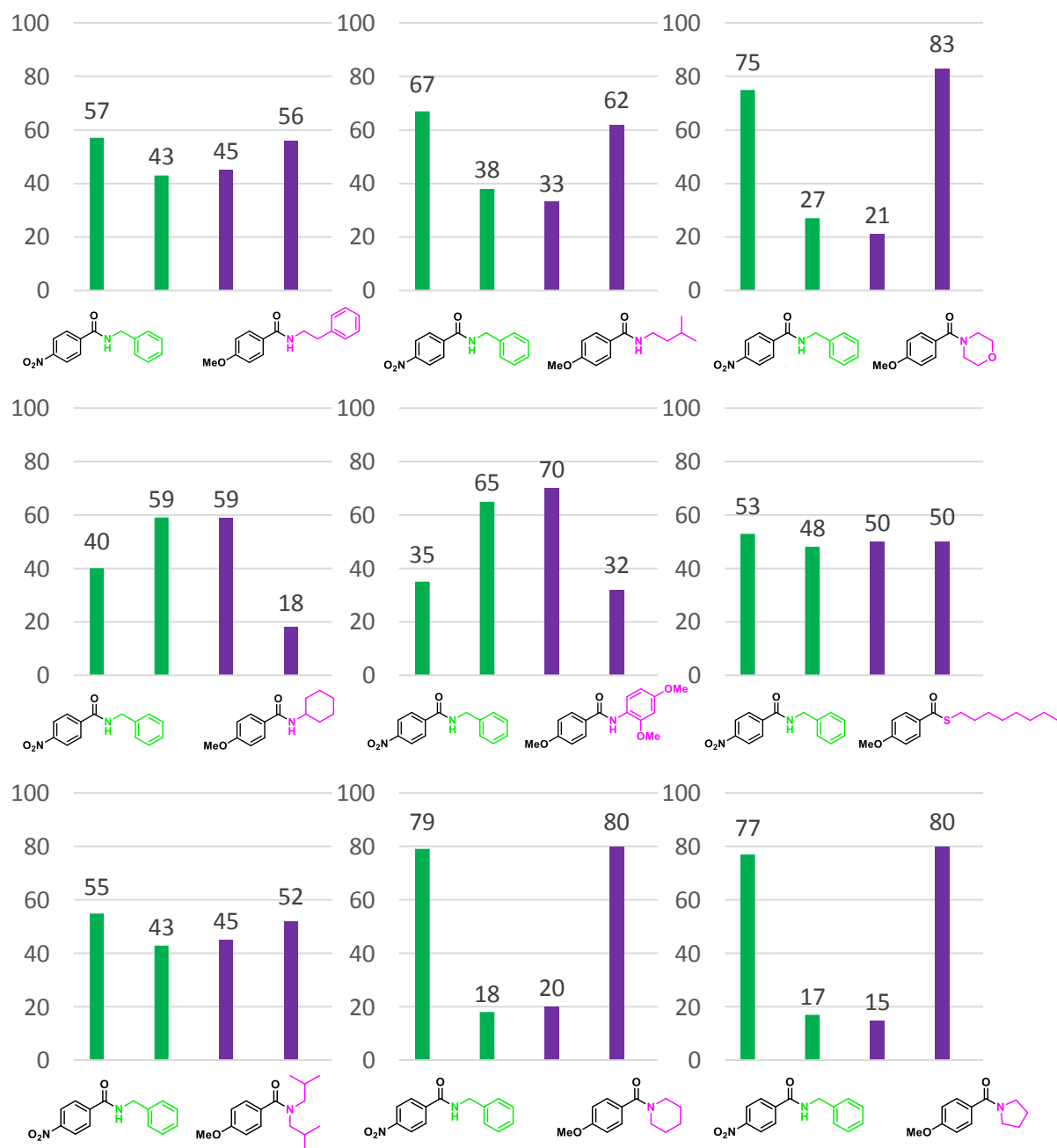


Figure 3.9 continued Self-sorting in $[2 \times 2]$ systems with fixed two acyl chlorides **35**, **36**, and benzylamine **37** while varying the other nucleophile (purple substrate). Only major compounds are shown.

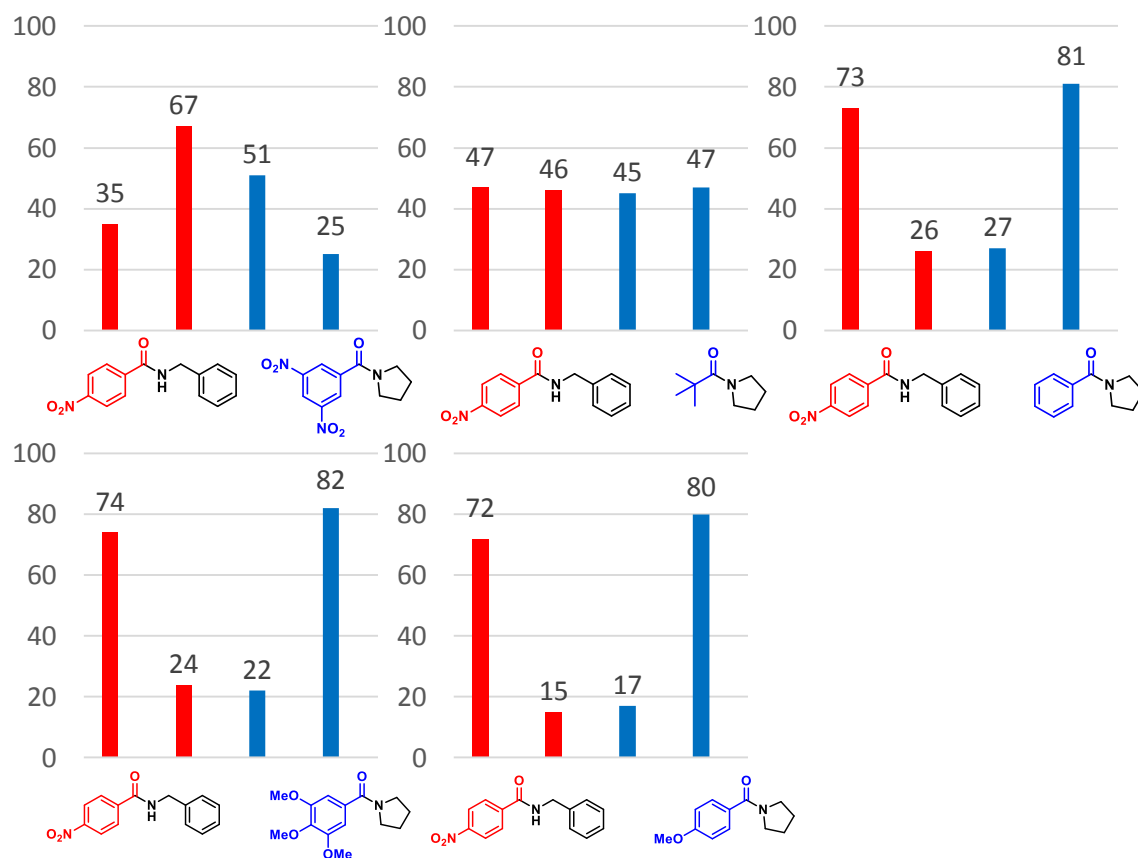
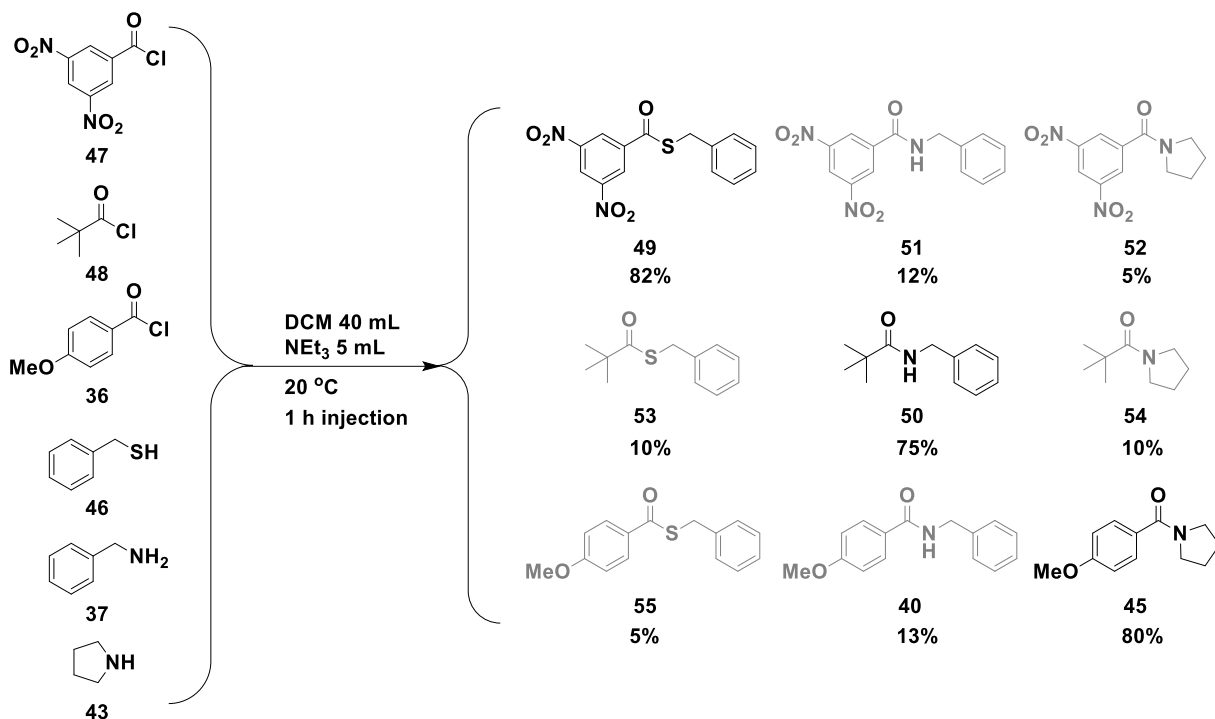


Figure 3.10 Self-sorting in [2×2] systems with fixed two nucleophiles **37**, **43** and acyl chlorides **35** while varying the other acyl chloride (blue substrate). Only major compounds are shown.

3.4.4 Selected Self-sorting Experimental Procedure for a [3×3] Acylation Mixture



Equimolar amounts of 3,5-dinitrobenzoyl chloride **47** (235 mg, 1.00 mmol), pivaloyl chloride **48** (120 mg, 1.00 mmol), and *p*-methoxybenzoyl chloride **36** (170 mg, 1.00 mmol), were mixed in anhydrous DCM (5 mL) and then transferred into a 5 mL syringe. Benzylamine **37** (107 mg, 1.00 mmol), pyrrolidine **43** (71 mg, 1.00 mmol), and benzyl mercaptan **46** (125 mg, 1.00 mmol) were mixed in anhydrous DCM (5 mL) and then transferred into another 5 mL syringe. Two syringes were placed into a syringe pump with injection rate set to 5 mL/h. A Schlenk flask (100 mL) was dried overnight in the oven and then backfilled with N₂, before anhydrous DCM (40 mL) and NEt₃ (5 mL) were added to it. The two syringes were connected to the Schlenk flask through two needles (20 G) and Teflon tubing. Four starting materials were then slowly injected at

room temperature to the solution in the flask over 1 h. After the reaction was finished, 2 mL out of 55 mL solution were used for characterization by NMR spectroscopy with trimethoxybenzene (12.1 mg, 0.074 mmol) as an internal standard. ^1H NMR analysis showed the identity of products as a mixture of 3,5-dinitro-thiobenzoic-acid-S-benzyl ester **49** (82% yield), benzyl 3,5-dinitrobenzamide **51** (12% yield), (3,5-dinitrophenyl)(pyrrolidin-1-yl)methanone **52** (5% yield), 2,2-dimethylthiopropionic acid S-benzyl ester **53** (10% yield), benzyl-2,2-dimethylpropionamide **50** (75% yield), 2,2-dimethyl-1-(pyrrolidin-1-yl)propan-1-one **54** (10% yield), 4-methyl-thiobenzoic acid S-benzyl ester **55** (5% yield), benzyl *p*-methoxybenzamide **40** (13% yield), and (*p*-methoxyphenyl)(pyrrolidin-1-yl)methanone **45** (80% yield).

3.4.5 Other Selective Acylation Self-Sorting in [3×3] Systems

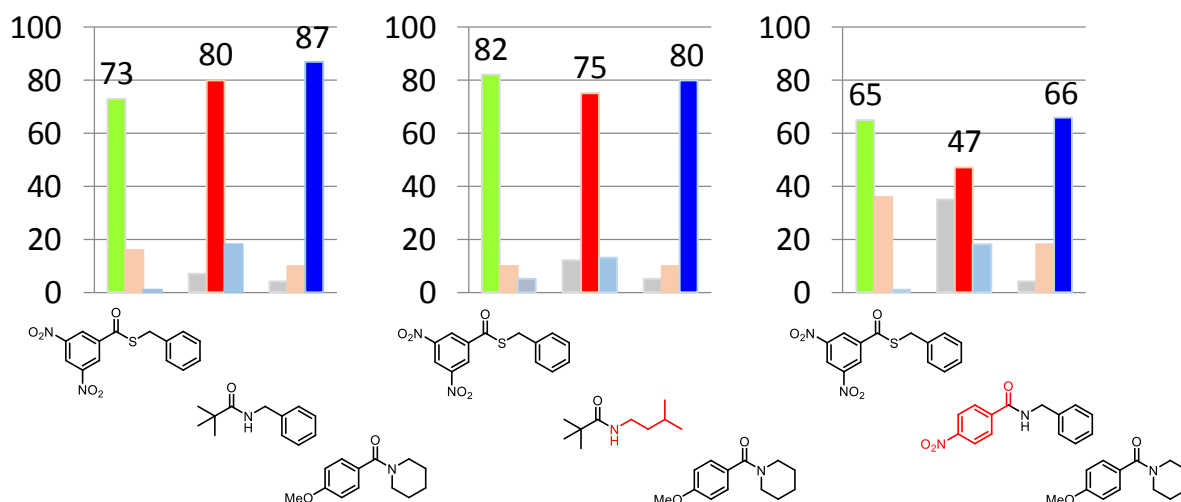


Figure 3.11 Selective self-sorting in [3×3] Systems, in which variations of substrate are indicated in red (comparing to the first example). Only major compounds are shown.

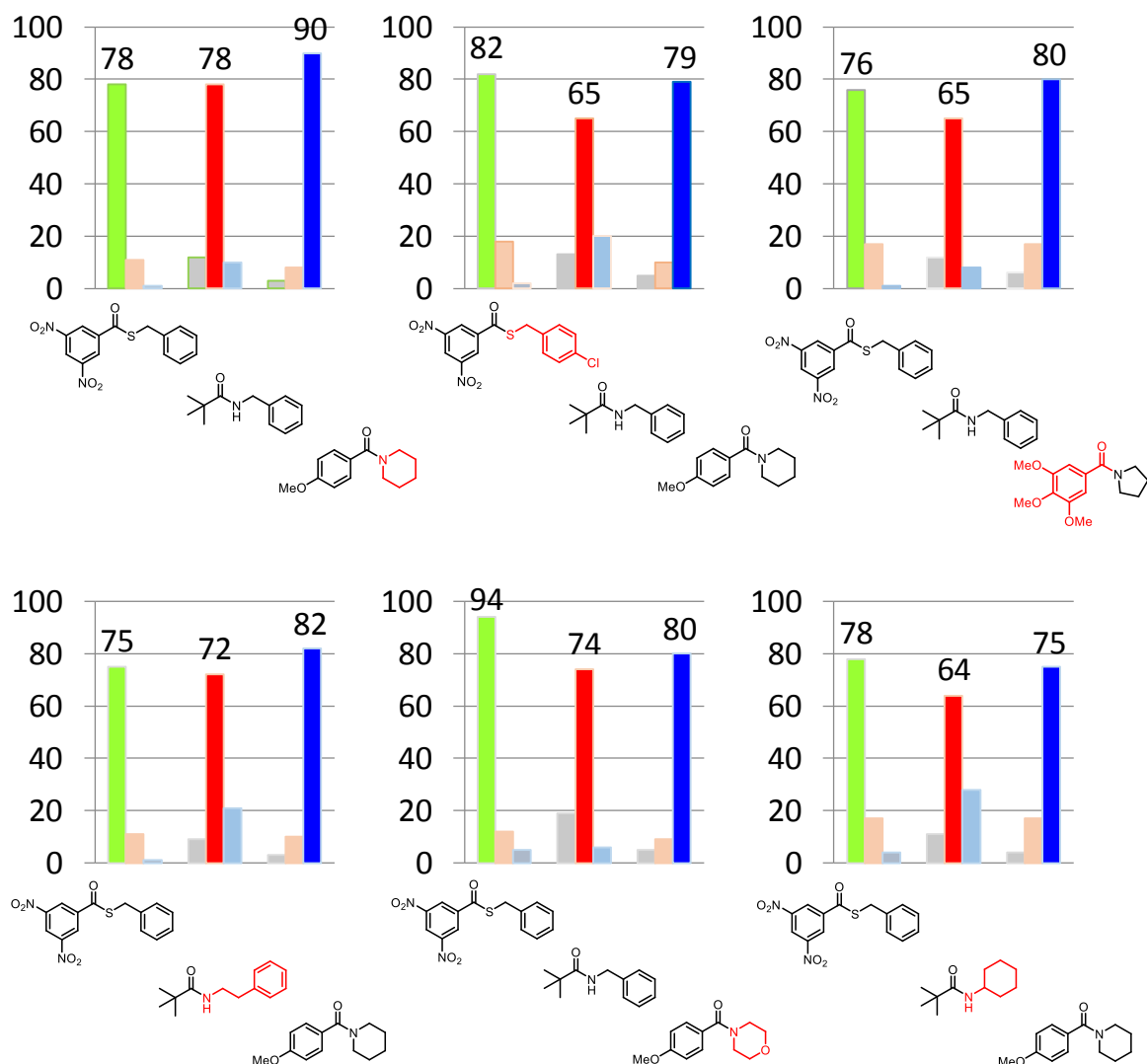


Figure 3.11 continued Selective self-sorting in [3x3] Systems, in which variations of substrate are indicated in red (comparing to the first example). Only major compounds are shown.

3.4.6 Synthesis of Individual Amides and Thioesters

3.4.6.1 General Procedure for Synthesis

Anhydrous DCM (40 mL) and NEt₃ (5 mL) were added to a Schlenk Flask (100 mL) which was pre-dried overnight in the oven and evacuated and backfilled with N₂. Compound **X** (2 mmol) was then dissolved in 5 mL of solvent DCM, and added into the solution using a 5 mL syringe with 20 G needle. Acyl chloride (2.2 mmol, 1.1 equiv.) was also dissolved in 5 mL DCM and injected dropwise into the flask. Reaction was stirred at 25 °C for 12 h. When the reaction was complete, the resulting mixture was extracted by deionized water (50 mL). The organic layer was concentrated under reduced pressure and further purified by column chromatography, affording analytically pure product (Table 3.1).

Table 3.1 Synthesized compound's structure, compound number, and production yield.

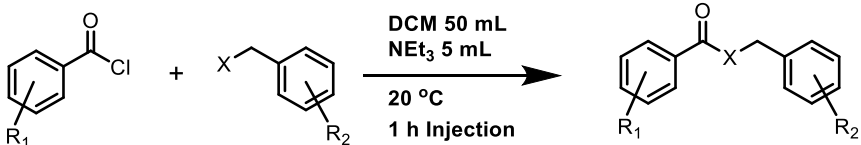
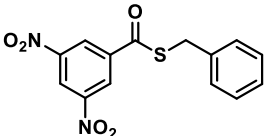
			
Entry	Compound Structure	Number	Yield
1		49	91%

Table 3.1 continued Synthesized compound's structure, compound number, and production yield.

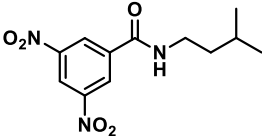
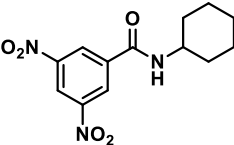
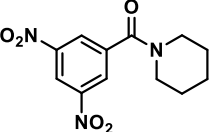
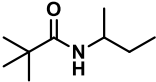
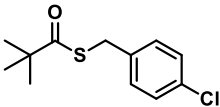
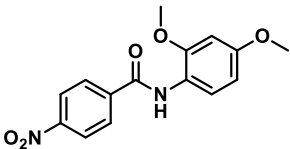
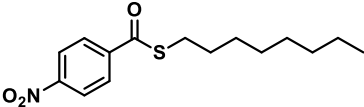
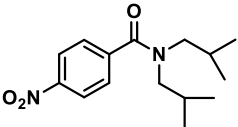
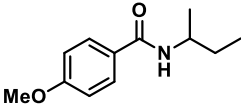
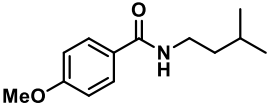
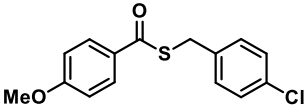
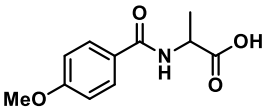
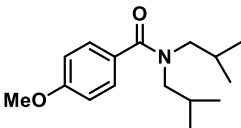
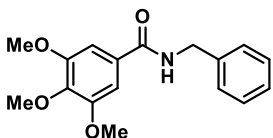
Entry	Compound Structure	Number	Yield
2		57	95%
3		58	89%
4		59	90%
5		61	84%
6		62	94%
7		63	86%
8		64	85%
9		66	91%

Table 3.1 continued Synthesized compound's structure, compound number, and production yield.

Entry	Compound Structure	Number	Yield
10		67	88%
11		68	94%
12		69	97%
13		71	76%
14		72	90%
15		73	89%

3.4.6.2 Compound Characterization

3,5-dinitro-thiobenzoic acid S-benzyl ester (**49**)

Compound **49** in 91% yield (542 mg, 1.88 mmol) with m.p. 121 °C. IR (neat): 3103 (w, $\tilde{\nu}_{C-H}$), 3080 (w, $\tilde{\nu}_{C-C}$), 1659 (m), 1624 (w), 1595 (w), 1537 (m), 1495 (w), 1340 (m),

1220 (w), 1111 (w), 989 (m), 926 (w) cm^{-1} . ^1H NMR (CDCl_3 , 500 MHz): δ 9.21 (t, $^3J_{\text{H-H}} = 2$ Hz, 1H), 9.07 (d, $^3J_{\text{H-H}} = 2$ Hz, 2H), 7.34 (m, 5H), 4.41 (s, 3H) ppm. ^{13}C NMR (CDCl_3 , 125 MHz): δ 187.48, 148.82, 139.63, 135.96, 129.14, 129.016, 128.08, 127.07, 122.46, 34.36 ppm.

N-isopentyl-3,5-dinitro-benzamide (57)

Compound **57** in 95% yield (495 mg, 1.92 mmol) with m.p. 140 °C. IR (neat): 3291 (m, $\tilde{\nu}_{\text{N-H}}$), 3103 (w, $\tilde{\nu}_{\text{C-H}}$), 2957 (m), 2873 (w), 1644 (m), 1537 (s), 1455 (w), 1340 (s), 1305 (w), 714 (m), 691 (m) cm^{-1} . ^1H NMR (CDCl_3 , 500 MHz): δ 9.16 (t, $^3J_{\text{H-H}} = 2$ Hz, 1H), 8.93 (d, $^3J_{\text{H-H}} = 2$ Hz, 2H), 6.36 (m, 1H), 3.55 (m, $^3J_{\text{H-H}} = 3$ Hz, 2H) ppm, 1.70 (m, 1H), 1.56 (m, 2H), 0.97 (d, $^3J_{\text{H-H}} = 6.9$ Hz, 6H) ppm. ^{13}C NMR (CDCl_3 , 125 MHz): δ 162.75, 148.73, 138.25, 127.18, 121.10, 39.23, 38.37, 26.04, 22.52 ppm.

cyclohexylamin-3,5-dinitrobenzoyl-derivat (58)

Compound **58** in 89% yield (464 mg, 1.90 mmol) with m.p. 132 °C. IR (neat): 3084 (w, $\tilde{\nu}_{\text{N-H}}$), 2949 (w, $\tilde{\nu}_{\text{C-H}}$), 2855 (w), 2873 (w), 1624 (m), 1547 (s), 1538 (s), 1474 (w), 1435 (w), 1343 (s), 1276 (m), 912 (m), 717 (m) cm^{-1} . ^1H NMR (CDCl_3 , 500 MHz): δ 9.06 (t, $^3J_{\text{H-H}} = 2.3$ Hz, 1H), 8.56 (d, $^3J_{\text{H-H}} = 2.3$ Hz, 2H), 3.74 (s, 2H), 3.34 (s, 2H), 1.63 (m, 7H) ppm. ^{13}C NMR (CDCl_3 , 125 MHz): δ 165.20, 148.56, 139.89, 127.40, 119.52, 49.06, 43.76, 26.62, 25.46, 24.33 ppm.

1-(3,5-dinitro-benzoyl)-piperidine (59)

Compound **59** in 90% yield (445 mg, 1.90 mmol) with m.p. 185 °C. IR (neat): 3036 (w, $\tilde{\nu}_{\text{C-H}}$), 1632 (s), 1549 (m), 1536 (s), 1435 (m), 1344 (s), 1281 (m), 1264 (w), 1109 (s), 1031 (m), 755 (m), 724 (s) cm^{-1} . ^1H NMR (CDCl_3 , 500 MHz): δ 9.15 (t, $^3J_{\text{H-H}} = 1.7$ Hz, 1H), 8.59 (d, $^3J_{\text{H-H}} = 1.7$ Hz, 2H), 3.68 (m, 10H) ppm. ^{13}C NMR (CDCl_3 , 125 MHz): δ 165.35, 148.66, 138.75, 127.64, 119.96, 66.68, 48.35, 43.01 ppm.

N-sec-butylpivaloylamide (61)

Compound **61** in 84% yield (261 mg, 1.80 mmol) with m.p. 101 °C. IR (neat): 3327 (m, $\tilde{\nu}_{\text{N-H}}$), 2965 (w, $\tilde{\nu}_{\text{C-H}}$), 2927 (w), 2872 (w), 1631 (s), 1536 (s), 1538 (s), 1447 (w), 1364 (m), 1296 (w), 1208 (m), 666 (m) cm^{-1} . ^1H NMR (CDCl_3 , 500 MHz): δ 5.33 (br, 1H), 3.88 (m, 1H), 1.42 (m, 2H), 1.17 (s, 9H), 1.09 (d, $^3J_{\text{H-H}} = 6.3$ Hz, 3H), 0.88 (t, $^3J_{\text{H-H}} = 6.3$ Hz, 3H) ppm. ^{13}C NMR (CDCl_3 , 125 MHz): δ 46.32, 38.68, 29.83, 27.71, 20.60, 10.42 ppm.

trimethyl ethyl acid S-(4-chloro-benzyl ester) (62)

Compound **62** in 94% yield (455 mg, 1.88 mmol) is liquid. IR (neat): 3115 (w), 1643 (m), 1602 (w), 1521 (m), 1488 (w), 1402 (w), 1348 (m), 1319 (m), 1192 (m), 1095 (m), 923 (m), 819 (m), 718 (s) cm^{-1} . ^1H NMR (CDCl_3 , 500 MHz): δ 8.29 (d, $^3J_{\text{H-H}} = 9.2$ Hz, 2H), 8.10 (d, $^3J_{\text{H-H}} = 9.2$ Hz, 2H), 7.33 (m, 4H), 4.31 (s, 2H) ppm. ^{13}C NMR (CDCl_3 , 125 MHz): δ 189.68, 141.27, 135.37, 130.45, 129.02, 128.42, 124.04, 33.21 ppm.

4-nitro-N-(2,4-dimethoxyphenyl)benzamide (63)

Compound **63** in 86% yield (491 mg, 1.90 mmol) with m.p. 169 °C. IR (neat): 3431 (w), 2927 (w, $\tilde{\nu}_{C-H}$), 2839 (w), 2873 (w), 1677 (m), 1602 (w), 1516 (s), 1500 (m), 1420 (w), 1340 (m), 1251 (w), 1212 (m), 1155 (m), 1031 (m), 851 (m), 705 (s) cm^{-1} . ^1H NMR (CDCl_3 , 500 MHz): δ 8.35 (m, 2H), 8.33 (d, $^3J_{H-H} = 8.6$ Hz, 2H), 8.03 (d, $^3J_{H-H} = 8.6$ Hz, 2H), 6.52 (m, 2H), 3.90 (s, 3H), 3.81 (s, 3H) ppm. ^{13}C NMR (CDCl_3 , 125 MHz): δ 162.83, 157.16, 149.65, 141.01, 128.25, 124.07, 120.94, 120.74, 103.95, 98.78, 55.99, 55.68 ppm.

S-octyl 4-nitrobenzothioate (64)

Compound **64** in 85% yield transparent liquid (447 mg, 1.70 mmol). IR (neat): 2924 (m, $\tilde{\nu}_{C-H}$), 2853 (w), 1663 (m), 1604 (w), 1525 (s), 1347 (s), 1200 (m), 920 (s), 861 (w), 847 (s), 718 (w), 692 (s) cm^{-1} . ^1H NMR (CDCl_3 , 500 MHz): δ 8.25 (m, $^3J_{H-H} = 8.6$ Hz, 2H), 8.07 (d, $^3J_{H-H} = 8.6$ Hz, 2H), 3.06 (t, $^3J_{H-H} = 7.4$ Hz, 2H), 1.63 (m, 2H), 1.39 (m, 2H), 1.24 (m, 8H) ppm. ^{13}C NMR (CDCl_3 , 125 MHz): δ 190.55, 150.46, 141.82, 128.23, 123.88, 31.85, 29.68, 29.38, 29.22, 29.15, 28.99, 22.71, 14.16 ppm.

diisobutylamin-4-nitrobenzamide (66)

Compound **66** in 91% yield (530 mg, 1.82 mmol) with m.p. 62 °C. IR (neat): 2960 (w, $\tilde{\nu}_{C-H}$), 2868 (w), 1626 (s), 1597 (m), 1518 (s), 1491 (w), 1383 (w), 1346 (s), 1268 (m), 1099 (m), 921 (w), 866 (w), 853 (w), 728 (m) cm^{-1} . ^1H NMR (CDCl_3 , 500 MHz): δ 8.25 (d, $^3J_{H-H} = 8.6$ Hz, 2H), 7.51 (d, $^3J_{H-H} = 8.6$ Hz, 2H), 3.37 (d, $^3J_{H-H} = 7.4$ Hz, 2H), 3.02 (d,

$^3J_{\text{H-H}} = 8.6$ Hz, 2H), 2.10 (m, 1H), 1.85 (m, 1H), 0.99 (d, $^3J_{\text{H-H}} = 6.3$ Hz, 6H), 0.74 (d, $^3J_{\text{H-H}} = 6.3$ Hz, 6H) ppm. ^{13}C NMR (CDCl_3 , 125 MHz): δ 170.20, 148.03, 143.77, 128.10, 123.92, 56.55, 51.28, 26.935, 26.26, 20.26, 19.86 ppm.

4-methoxy-N-sek.butyl-benzamid (67)

Compound **67** in 88% yield (363 mg, 1.96 mmol) with m.p. 101 °C. IR (neat): 3318 (w), 2968 (w, $\tilde{\nu}_{\text{C-H}}$), 1629 (w), 1608 (m), 1533 (m), 1505 (s), 1454 (w), 1307 (w), 1250 (m), 1174 (m), 1026 (m), 841 (s), 788 (w), 770 (w), 672 (m) cm^{-1} . ^1H NMR (CDCl_3 , 500 MHz): δ 7.71 (d, $^3J_{\text{H-H}} = 8.6$ Hz, 2H), 6.90 (d, $^3J_{\text{H-H}} = 8.6$ Hz, 2H), 5.85 (d, 1H), 4.10 (m, 1H), 3.82 (s, 3H), 1.55 (m, 1H), 1.20 (d, $^3J_{\text{H-H}} = 6.8$ Hz, 3H), 0.94 (t, $^3J_{\text{H-H}} = 7.5$ Hz, 3H) ppm. ^{13}C NMR (CDCl_3 , 125 MHz): δ 166.49, 162.05, 128.66, 127.41, 113.75, 55.48, 47.06, 29.94, 20.67, 10.54 ppm.

N-isopentyl-4-methoxy-benzamid (68)

Compound **68** in 94% yield (520 mg, 1.88 mmol) as liquid. IR (neat): 3305 (w, $\tilde{\nu}_{\text{N-H}}$), 2954 (w, $\tilde{\nu}_{\text{C-H}}$), 2869 (w), 1627 (m), 1605 (m), 1544 (w), 1504 (m), 1463 (w), 1296 (w), 1251 (s), 1213 (m), 1177 (m), 1030 (m), 843 (m), 767 (w) cm^{-1} . ^1H NMR (CDCl_3 , 500 MHz): δ 7.71 (d, $^3J_{\text{H-H}} = 8.6$ Hz, 2H), 6.83 (d, $^3J_{\text{H-H}} = 8.6$ Hz, 2H), 7.26 (d, $^3J_{\text{H-H}} = 8.0$ Hz, 2H), 6.54 (br, 1H), 3.77 (s, 3H), 3.38 (m, 2H) 1.61 (m, 1H), 1.44 (d, $^3J_{\text{H-H}} = 6.3$ Hz, 6H) ppm. ^{13}C NMR (CDCl_3 , 125 MHz): δ 167.24, 162.02, 128.79, 127.17, 113.67, 55.41, 38.61, 38.44, 26.03, 22.57 ppm.

4-methoxybenzoic acid S-(4-chloro-benzyl ester) (69)

Compound **69** in 97% yield (535 mg, 1.94 mmol) with m.p. 54 °C. IR (neat): 2930 (w, $\tilde{\nu}_{C-H}$), 2837 (w), 1648 (m), 1595 (m), 1533 (m), 1506 (w), 1482 (w), 1460 (w), 1441 (w), 1256 (m), 1213 (m), 1162 (m), 1086 (w), 915 (s), 727 (w) cm^{-1} . ^1H NMR (CDCl_3 , 500 MHz): δ 7.93 (d, $^3J_{H-H} = 9.1$ Hz, 2H), 7.30 (d, $^3J_{H-H} = 8.0$ Hz, 2H), 7.26 (d, $^3J_{H-H} = 8.0$ Hz, 2H), 6.92 (d, $^3J_{H-H} = 9.1$ Hz, 2H), 4.24 (s, 2H), 3.85 (s, 3H) ppm. ^{13}C NMR (CDCl_3 , 125 MHz): δ 189.59, 164.01, 136.59, 133.13, 130.41, 129.61, 129.53, 128.82, 113.92, 55.63, 32.54 ppm.

diisobutylamin-4-methoxybenzamide (72)

Compound **72** in 90% yield (430 mg, 1.80 mmol) is liquid. IR (neat): 2957 (w, $\tilde{\nu}_{C-H}$), 2870 (w), 1625 (m), 1608 (m), 1511 (w), 1460 (w), 1367 (m), 1297 (w), 1247 (s), 1170 (m), 1099 (m), 1029 (m), 838 (w), 767 (w) cm^{-1} . ^1H NMR (CDCl_3 , 500 MHz): δ 7.27 (d, $^3J_{H-H} = 8.6$ Hz, 2H), 6.84 (d, $^3J_{H-H} = 8.0$ Hz, 2H), 3.76 (s, 3H), 3.19 (d, $^3J_{H-H} = 91.0$ Hz, 4H), 1.92 (d, $^3J_{H-H} = 130.6$ Hz, 2H), 0.80 (d, $^3J_{H-H} = 181.6$ Hz, 6H) ppm. ^{13}C NMR (CDCl_3 , 125 MHz): δ 172.53, 160.20, 129.74, 128.91, 113.65, 56.90, 55.33, 51.37, 26.88, 26.27, 20.24, 19.86 ppm.

N-benzyl-3,4,5-trimethoxybenzamide (73)

Compound **73** in 89% yield (535 mg, 1.78 mmol) with m.p. 139 °C. IR (neat): 3303 (w, $\tilde{\nu}_{C-H}$), 2941 (w), 1624 (m), 1578 (m), 1526 (w), 1496 (w), 1325 (w), 1297 (w), 1231 (m), 1123 (s), 991 (w), 840 (w), 751 (m) cm^{-1} . ^1H NMR (CDCl_3 , 500 MHz): δ 7.33 (m, 5H),

7.01 (s, 2H), 6.36 (br, 1H), 4.64 (d, $^3J_{\text{H-H}} = 5.7$ Hz, 2H), 3.88 (s, 6H), 3.87 (s, 3H) ppm.

^{13}C NMR (CDCl_3 , 125 MHz): δ 167.11, 153.31, 138.26, 129.87, 128.91, 128.07, 127.78, 104.42, 61.02, 56.44, 44.35 ppm.

3.4.7 Experimental Apparatus

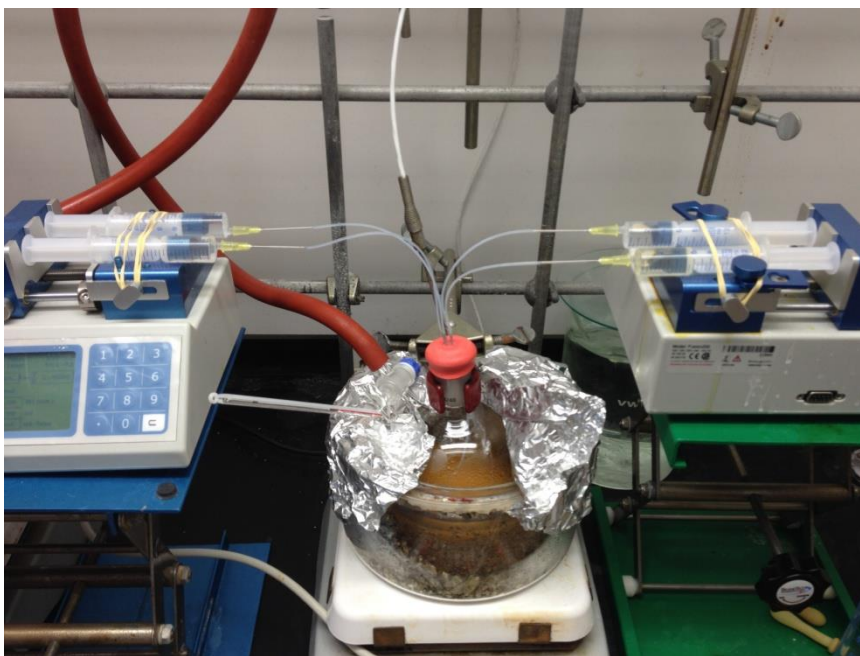


Figure 3.12 Reaction system constructed from two injection pumps, cooling bath (isopropanol with dry ice), and N_2 protecting atmosphere. Two acyl chlorides were put in the syringe on the left while two nucleophiles on the right. All of the syringes were injected at the same time and same rate.

Reference

- [1] Batten, S. R.; Champness, N. R.; Chen, X.; Garcia-Martinez, J.; Kitagawa, S.; O'Keeffe, M.; Suh, M. P.; Reedijk J. *Pure Appl. Chem.* **2013**, 85, 1715–1724.
- [2] Yaghi, O. M.; Li, G. M.; Li, H. L. *Nature* **1995**, 378, 703–706.
- [3] Li, H.; Eddaoudi, M.; O'Keeffe, M.; Yaghi, O. M. *Nature* **1999**, 402, 276–279.
- [4] Chui, S. S.-Y.; Lo, S. M.-F.; Charmant, J. P. H.; Orpen, A. G.; Williams, I. D. *Science*, **1999**, 283, 1148–1150.
- [5] (a) Suh, M. P.; Park, H. J.; Prasad, T. K.; Lim, D. W. *Chem. Rev.* **2012**, 112, 782–835. (b) Li, J. R.; Ma, Y. G.; McCarthy, M. C.; Sculley, J.; Yu, J. M.; Jeong, H. K.; Balbuena, P. B.; Zhou, H. C. *Chem. Rev.* **2011**, 255, 1791–1823.
- [6] (a) Li, J. R.; Kuppler, R. J.; Zhou, H. C. *Chem. Soc. Rev.* **2009**, 38, 1477–1504. (b) Li, J. R.; Sculley, J.; Zhou, H. C. *Chem. Rev.* **2012**, 112, 869–932. (c) Chen, J.; Zhang, J.; Li, J.; Fu, F.; Yang, H.-H.; Chen, G. *Chem. Commun.* **2010**, 46, 5939–5941.
- [7] (a) Seo, J. S.; Whang, D.; Lee, H.; Jun, S. I.; Oh, J.; Jeon, Y. J.; Kim, K. *Nature* **2000**, 404, 982–986. (b) Dybtsev, D. N.; Nuzhdin, A. L.; Chun, H.; Bryliakov, K. P.; Talsi, E. P.; Fedin, V. P.; Kim, K. *Angew. Chem. Int. Ed.* **2006**, 45, 916–920. (c) Wu, C. D.; Hu, A.; Zhang, L.; Lin, W. B. *J. Am. Chem. Soc.* **2005**, 127, 8940–8941. (d) Farrusseng, D.; Aguado, S.; Pinel, C. *Angew. Chem. Int. Ed.* **2009**, 48, 7502–7513. (e) Hwang, I. H.; Bae, J. M.; Kim, W.-S.; Jo, Y. D.; Kim, C.; Kim, Y.; Kim, S.-J.; Huh, S. *Dalton Trans.* **2012**, 41, 12759–12765. (f) Lee, J.; Farha, O. K.; Roberts, J.; Scheidt, K. A.; Nguyen, S. T.; Hupp, J. T. *Chem. Soc. Rev.* **2009**,

- 38, 1450–1459. (g) Farha, O. K.; Shultz, A. M.; Sarjeant, A. A.; Nguyen, S. T.; Hupp, J. T. *J. Am. Chem. Soc.* **2011**, *133*, 5652–5655.
- [8] James, S. L. *Chem. Soc. Rev.* **2003**, *32*, 276–288.
- [9] Horcajada, P.; Chalati, T.; Serre, C.; Gillet, B.; Sebrie, C.; Baati, T.; Eubank, J. F.; Heurtaux, D.; Clayette, P.; Kreuz, C.; Chang, J. S.; Hwang, Y. K.; Marsaud, V.; Bories, P. N.; Cynober, L.; Gil, S.; Ferey, G.; Couvreur, P.; Gref, R. *Nat. Mater.* **2010**, *9*, 172–178.
- [10] Parnham, E. R.; Morris, R. E. *Acc. Chem. Res.* **2007**, *40*, 1005–1013.
- [11] (a) Wang, Z.; Cohen, S. M. *Chem. Soc. Rev.* **2009**, *38*, 1315–1329. (b) Tanabe, K. K.; Cohen, S. M. *Chem. Soc. Rev.* **2011**, *40*, 498–519.
- [12] Karagiari, O.; Bury, W.; Tylianakis, E.; Sarjeant, A. A.; Hupp, J. T.; Farha, O. K. *Chem. Mater.* **2013**, *25*, 3499–3503.
- [13] Nguyen, J. G.; Cohen, S. M. *J. Am. Chem. Soc.* **2010**, *132*, 4560–4561.
- [14] Sela, M.; Lifson, S. *Biochim. Biophys. Acta.* **1959**, *36*, 471–478.
- [15] Otto, S.; Furlan, R. L. E.; Sanders, J. K. M. *J. Am. Chem. Soc.* **2000**, *122*, 12063–12064.
- [16] Otto, S.; Furlan, R. L. E.; Sanders, J. K. M. *Science* **2002**, *297*, 590–593.
- [17] Corbett, P. T.; Sanders, J. K. M.; Otto, S. *J. Am. Chem. Soc.* **2005**, *127*, 9390–9392.
- [18] Jiang, Y.; Qin, Y.; Xie, S.; Zhang, X.; Dong, J.; Ma, D. *Org. Lett.* **2009**, *11*, 5250–5253.

- [19] Takeda, K.; Kuwahara, A.; Ohmori, K.; Takeuchi, T. *J. Am. Chem. Soc.* **2009**, *131*, 8833–8838.
- [20] Lukesh, J. C.; Palte, M. J.; Raines, R. T. *J. Am. Chem. Soc.* **2012**, *134*, 4057–4059.
- [21] Jiang, Y.; Qin, Y.; Xie, S.; Zhang, X.; Dong, J.; Ma, D. *Org. Lett.* **2009**, *11*, 5250–5253.
- [22] Takeda, K.; Kuwahara, A.; Ohmori, K.; Takeuchi, T. *J. Am. Chem. Soc.*, **2009**, *131*, 8833–8838.
- [23] Raimon, P.; Gimenez, L.; Pettersson, S.; Pascual, R.; Gonzalo, E.; Este, J. A.; Clotet, B.; Borrell, J. I.; Teixido, J. *Eur. J. Med. Chem.* **2012**, *54*, 159–174.
- [24] Wade, C. R.; Li, M.; Dincă, M. *Angew. Chem. Int. Ed.* **2013**, *52*, 13377–13381.
- [25] Cheng, G.; Hasell, T.; Trewin, A.; Adams, D. J.; Cooper, A. I. *Angew. Chem. Int. Ed.* **2012**, *51*, 7892–7894.
- [26] Aoyama, Y. *Top. Curr. Chem.* **1998**, *198*, 131–161.
- [27] Simard, M.; Su, D.; Wuest, J. D. *J. Am. Chem. Soc.* **1991**, *113*, 4696–4698.
- [28] He, Y.; Xiang, S.; Chen, B. *J. Am. Chem. Soc.* **2011**, *133*, 14570–14573.
- [29] Cooper, A. I. *Angew. Chem. Int. Ed.* **2012**, *51*, 7982–7984.
- [30] Yang, W.; Greenaway, A.; Lin, X.; Matsuda, R.; Blake, A. J.; Wilson, C.; Lewis, W.; Hubberstey, P.; Kitagawa, S.; Champness, N. R.; Schroder, M. *J. Am. Chem. Soc.* **2010**, *132*, 14457–14469.
- [31] Brunet, P.; Simard, M.; Wuest, J. D. *J. Am. Chem. Soc.* **1997**, *119*, 2737–2738.

- [32] (a) Ananchenko, G. S.; Moudrakovski, I. L.; Coleman, A. W.; Ripmeester, J. A. *Angew. Chem. Int. Ed.* **2008**, *47*, 5616–5618. (b) Atwood, J. L.; Barbour, L. J.; Jerga, A. *Science* **2002**, *296*, 2367–2369.
- [33] (a) Tozawa, T.; *et al.* *Nat. Mater.* **2009**, *8*, 973–978. (b) Mastalerz, M.; Schneider, M. W.; Oppel, I. M.; Presly, O. *Angew. Chem. Int. Ed.* **2011**, *50*, 1046–1051.
- [34] Tranchemontagne, D. J. L.; Ni, Z.; O'Keeffe, M.; Yaghi, O. M. *Angew. Chem. Int. Ed.* **2008**, *47*, 5136–5147.
- [35] Bezzu, C. G.; Helliwell, M.; Warren, J. E.; Allan, D. R.; McKeown, N. B. *Science* **2010**, *327*, 1627–1630.
- [36] Lv, J.; Perez–Krap, C.; Suyetin, M.; Alsmail, N. H.; Yan, Y.; Yang, S.; Lewis, W.; Bichoutskaia, E.; Tang, C.; Blake, A. J.; Cao, R.; Schröder, M.; *J. Am. Chem. Soc.* **2014**, *136*, 12828–12831.
- [37] Chen, T.; Popov, I.; Kaveevivitchai, W.; Chuang, Y.; Chen, Y.; Daugulis, O.; Jacobson, A. J.; Miljanić, O. Š. *Nat. Commun.* **2014**, *5*, 5131.
- [38] Le, H. T. M.; El-Hamdi, N.; Miljanić, O. Š. *J. Org. Chem.* **2015**, *80*, 5210–5217.
- [39] Do, H.; Daugulis, O. *J. Am. Chem. Soc.* **2011**, *133*, 13577–13586.
- [40] Dolbier, W.R.; Xie, P.; Zhang, L.; Xu, W.; Chang, Y.; Abboud, K. A. *Org. Lett.* **2008**, *73*, 2469–2472.
- [41] Wu, A.; Isaacs, L. *J. Am. Chem. Soc.* **2003**, *125*, 4831–4835.
- [42] Caulder, D. L.; Raymond, K. N. *Angew. Chem. Int. Ed.* **1997**, *36*, 1440–1441.
- [43] Jolliffe, K. A.; Timmerman, P.; Reinhoudt, D. N. *Angew. Chem. Int. Ed.* **1999**, *38*, 931–933.

- [44] Rowan, S. J.; Hamilton, D. G.; Brady, P. A.; Sanders, J. K. M. *J. Am. Chem. Soc.* **1997**, *119*, 2578–2579.
- [45] Watson, J. D.; Crick, F. H. *Nature* **1953**, *171*, 737–738.
- [46] Reek, J. N. H.; Otto, S. Wiley-VCH: Weinheim, **2010**.
- [47] Corbett, P. T.; Leclaire, J.; Vial, L.; West, K. R.; Wietor, J. L.; Sanders, J. K. M.; Otto, S. *Chem. Rev.* **2006**, *106*, 3652–3711.
- [48] Ji, Q.; Lirag, R. C.; Miljanić, O. Š. *Chem. Soc. Rev.* **2014**, *43*, 1873–1884.
- [49] Ji, Q.; Miljanić, O. Š. *J. Org. Chem.* **2013**, *78*, 12710–12716.